Gene knock-ins in *Drosophila* using homology-independent insertion of universal donor plasmids

Justin A. Bosch[1], Ryan Colbeth[1], Jonathan Zirin[1], Norbert Perrimon[1,2]

[1] Department of Genetics, Harvard Medical School, Boston, MA, 02115, USA

[2] Howard Hughes Medical Institute, Boston, MA, 02115, USA

Short Running Title: Homology-independent knock-ins in flies

Keywords: CRISPR-Cas9, knock-in, homology-independent, gene function, CRISPaint

100-word article summary: We report a new homology-independent genomic knock-in method in *Drosophila* to insert large DNA elements into any target gene. Using CRISPR-Cas9 and non-homologous end joining (NHEJ), an entire donor plasmid is inserted into the genome without the need for homology arms. This approach eliminates the burden associated with designing and constructing traditional donor plasmids. We demonstrate its usefulness in cultured cells and in vivo to fluorescently tag endogenous proteins, generate reporters of gene expression, and disrupt gene function.

Corresponding author:

Norbert Perrimon

Harvard Medical School

77 Avenue Louis Pasteur

Dept. of Genetics, NRB 336

Boston, MA 02115

617-432-7672

Email: perrimon@genetics.med.harvard.edu

Abstract

Site-specific insertion of DNA into endogenous genes (knock-in) is a powerful method to study gene function. However, traditional methods for knock-in require laborious cloning of long homology arms for homology-directed repair. Here, we report a simplified method in *Drosophila melanogaster* to insert large DNA elements into any gene using homology-independent repair. This method, known as CRISPaint, employs CRISPR-Cas9 and non-homologous end joining (NHEJ) to linearize and insert donor plasmid DNA into a target genomic cut site. The inclusion of commonly used elements such as GFP on donor plasmids makes them universal, abolishing the need to create gene-specific homology arms and greatly reducing user workload. Using this method, we show robust gene-specific integration of donor plasmids in cultured cells and the fly germ line. Furthermore, we use this method to analyze gene function by fluorescently tagging endogenous proteins, disrupting gene function, and generating reporters of gene expression. Finally, we assemble a collection of donor plasmids for germ line knock-in that contain commonly used insert sequences. This method simplifies the generation of site-specific large DNA insertions in *Drosophila* cell lines and fly strains, and better enables researchers to dissect gene function in vivo.

Introduction

Insertion of DNA into the animal genome is a powerful method to study gene function. This approach is multipurpose, and can be used to visualize protein localization (CRIVAT AND TARASKA 2012; HASSE *et al.* 2016; KANCA *et al.* 2017), to disrupt gene function (HOUSDEN *et al.* 2017), to assay gene expression (BRAND AND PERRIMON 1993; IVICS *et al.* 2009; BOUABE AND OKKENHAUG 2013), or to purify endogenous proteins (KIMPLE *et al.* 2013). Furthermore, the ability to insert large DNA elements such as promoters, protein coding sequences, or entire genes into the genome offers researchers endless options for genome modification. *Drosophila melanogaster* is an excellent animal model to analyze gene function because of its many genetic tools, fast generation time, and in vivo analysis (VENKEN *et al.* 2016; KORONA *et al.* 2017; BIER *et al.* 2018).

The two most commonly used methods in *Drosophila* to knock-in DNA into endogenous genes involve either transposable elements or homology directed-repair (HDR). Transposable DNA elements insert randomly in the genome by a Transposase enzyme (BELLEN *et al.* 2011), and cannot be used to target a user-specified gene. In contrast, HDR is used to insert DNA into a specific genomic location by cleavage at the genomic locus and precise homologous recombination of the DNA insert into the genome (BIER *et al.* 2018). Circular plasmids are commonly used as donor DNA for HDR because they can carry a large DNA insert (≤10kb) and homology arms corresponding to the target locus are added by traditional cloning techniques. While HDR is a useful method, the design and construction of unique plasmid donors for each gene is laborious. As a cloning-free alternative, synthesized single-stranded DNA (ssDNA) with short homology arms (~50-100 bp each) (BIER *et al.* 2018) or long

ssDNAs of ≤2kb (QUADROS *et al.* 2017) can be used as donors. However, ssDNA donors are limited to relatively small insertions such as epitope tags, and, like HDR plasmid donors, must be designed and produced for each gene that is targeted. Therefore, there is a need for easier, faster, and cheaper alternatives to knock-in large DNA elements into the *Drosophila* genome.

It was recently shown that large DNA elements could be knocked into a specific target locus without homology arms, known as homology-independent insertion (CRISTEA *et al.* 2013; MARESCA *et al.* 2013; AUER *et al.* 2014; KATIC *et al.* 2015; LACKNER *et al.* 2015; SCHMID-BURGK *et al.* 2016; SUZUKI *et al.* 2016; KATOH *et al.* 2017). In this method, simultaneous cutting of a circular donor plasmid and a genomic target-site by a nuclease such as Cas9 results in integration of the linearized donor plasmid into the genomic cut site by non-homologous end joining (NHEJ). This removes the need to construct homology arms, and only requires cloning or synthesizing a gene-specific single guide RNA (sgRNA). Furthermore, this approach is modular, since donor plasmids containing common insert sequences (e.g. GFP) can be targeted to different genomic locations and are thus “universal”. Generating knock-ins by homology-independent insertion has been successfully applied in human cell lines (CRISTEA *et al.* 2013; MARESCA *et al.* 2013; LACKNER *et al.* 2015; SCHMID-BURGK *et al.* 2016; KATOH *et al.* 2017), mouse somatic cells (SUZUKI *et al.* 2016), zebrafish (AUER *et al.* 2014), and *C. elegans* (KATIC *et al.* 2015). However, this approach has not yet been applied in *Drosophila*.

Here, we show that homology-independent insertion functions effectively in *Drosophila* by using the CRISPaint method. We first characterize this method in cultured S2R+ cells, showing that a universal mNeonGreen donor plasmid can be used to fluorescently tag endogenous proteins at their C-terminus. We then demonstrate that

126 this approach works *in vivo*, using a universal *T2A-Gal4* donor plasmid in the fly germ
127 line to obtain fly lines with insertions in a number of characterized genes. We show that
128 these insertions can be used as expression reporters for the target gene and to
129 generate loss-of-function phenotypes. Finally, we present a collection of different
130 universal donor plasmids for the purpose of enabling the *Drosophila* research
131 community to employ this method for their specific uses.
132
133 **Materials and Methods**
134
135 **Plasmid cloning**
136
137 *pCFD3-frame_selector_*(*0, 1, or 2*) plasmids (Addgene #s 127553-127555) were
138 cloned by ligating annealed oligos encoding sgRNAs that target the CRISPaint target
139 site (SCHMID-BURGK *et al.* 2016) into *pCFD3* (PORT *et al.* 2014), which contains the
140 *Drosophila U6:3* promoter.
141 Additional sgRNA-encoding plasmids were generated by the TRiP
142 (https://fgr.hms.harvard.edu/) or obtained from Filip Port (PORT *et al.* 2015). sgRNA
143 plasmids targeting CDS close to the stop codon were *GP07595* (*Act5c*), *GP07596*
144 (*His2Av*), *GP07609* (*alphaTub84B*), and *GP07612* (*Lam*). sgRNA plasmids targeting
145 CDS close to the start codon were *GP06461* (*wg*), *GP02894* (*FK506-bp2*), *GP05054*
146 (*alphaTub84B*), *GP00225* (*esg*), *GP00364* (*Myo1a*), *GP00400* (*btl*), *GP00583* (*Mhc*),
147 *GP01881* (*hh*), *GP03252* (*Desat1*), *GP05302* (*ap*), *pFP545* (*ebony*), and *pFP573*
148 (*ebony*). These sgRNAs were cloned into *pCFD3*, with the exception of those targeting
149 *esg*, *Myo1a*, *btl*, and *Mhc*, which were cloned into *pl100* (KONDO AND UEDA 2013).

150 *pCRISPaint-T2A-Gal4-3xP3-RFP* (Addgene # 127556) was constructed using
151 Gibson assembly (E2611, NEB) of three DNA fragments: 1) *Gal4-SV40-3xP3-RFP* was
152 PCR amplified from *pHD-Gal4-DsRed* (Xu et al. 2019 submitted PNAS, (GRATZ *et al.*
153 2014); 2) linear plasmid backbone generated by digesting *pWalium10-roe* (PERKINS *et*
154 *al.* 2015) with AscI/SacI; and 3) a synthesized double-stranded DNA fragment (gBlock,
155 IDT) encoding the CRISPaint target site, linker sequence, T2A, and ends that overlap
156 the other two fragments.
157 *pCRISPaint-T2A-ORF-3xP3-RFP* donor plasmids (Addgene #s 127557-127565)
158 were cloned by PCR amplifying the ORFs and Gibson cloning into *CRISPaint-T2A-*
159 *Gal4-3xP3-RFP* cut with NheI/KpnI. ORF sequences were amplified from templates as
160 follows: *sfGFP* [amplified from *pUAS-TransTimer* (He et al. 2019 submitted)], *LexGAD*
161 [amplified from p*CoinFLP-LexGAD/Gal4* (BOSCH *et al.* 2015)], *QF2* amplified from
162 Addgene #80274, *Cas9-T2A-GFP* (amplified from template kindly provided by Raghuvir
163 Viswanatha), *FLPo* (amplified from Addgene #24357), *Gal80* (amplified from Addgene
164 #17748), *Nluc* (amplified from Addgene #62057), *Gal4DBD*, (amplified from Addgene
165 #26233), and *p65* (amplified from Addgene #26234).
166 *pCRISPaint-sfGFP-3xP3-RFP* (Addgene # 127566) was cloned by PCR
167 amplifying *sfGFP* coding sequence and Gibson cloning into *CRISPaint-T2A-Gal4-3xP3-*
168 *RFP* cut with NotI/KpnI.
169 *pCRISPaint-CRIMIC_phase_*(*0,1, or 2*) (Addgene #s 127567-127569) donor
170 plasmids were cloned by ligating annealed oligos containing the CRISPaint target site
171 into *CRIMIC* [*pM37*, (LEE *et al.* 2018)] (frames 0,1,2) cut with NsiI.
172 *pCRISPaint-TGEM_phase_*(*0,1,or 2*) (Addgene #s 127570-127572) donor
173 plasmids were cloned by ligating annealed oligos containing the CRISPaint target site
174 into *T-GEM* (DIAO *et al.* 2015) (frames 0,1,2) cut with AgeI/NotI.

175 See Supplemental Table 6 for oligo and dsDNA sequences and Addgene for
176 plasmid sequences.
177
178 **Cell culture**
179
180 *Drosophila* S2R+ cells stably expressing Cas9 and a mCherry protein trap in *Clic*
181 (known as PT5/Cas9) (VISWANATHA *et al.* 2018) were cultured at 25˚C using Schneider's
182 media (21720-024, ThermoFisher) with 10% FBS (A3912, Sigma) and 50 U/ml penicillin
183 strep (15070-063, ThermoFisher). S2R+ cells were transfected using Effectene
184 (301427, Qiagen) following the manufacturer's instructions. Plasmid mixes were
185 composed of sgRNA-expressing plasmids (see above) and *pCRISPaint-mNeon-PuroR*
186 (SCHMID-BURGK *et al.* 2016). Cells were transfected with plasmid mixes in 6-well dishes
187 at $1.8x10^6$ cells/ml, split at a dilution of 1:6 after 3-4 days, and incubated with 2 µg/ml
188 Puromycin (540411 Calbiochem). Every 3-5 days, the media was replaced with fresh
189 Puromycin until the cultures became confluent (~12-16 days). For single-cell cloning
190 experiments, cultures were split 1:3 two days before sorting. Cells were resuspended in
191 fresh media, triturated to break up cell clumps, and pipetted into a cell straining FACS
192 tube (352235 Corning). Single cells expressing mNeonGreen were sorted into single
193 wells of a 96 well plate containing 50% conditioned media 50% fresh media using an
194 Aria-594 instrument at the Harvard Medical School Division of Immunology's Flow
195 Cytometry Facility. Once colonies were visible by eye (3-4 weeks), they were expanded
196 and screened for mNeonGreen fluorescence.
197
198 **Fly genetics and embryo injections**
199

200 Flies were maintained on standard fly food at 25˚C. Fly stocks were obtained
201 from the Perrimon lab collection or Bloomington Stock center (indicated with BL#).
202 Stocks used in this study are as follows: *yw* (Perrimon Lab), *yw/Y hs-hid* (BL8846), *yw;*
203 *nos-Cas9attP40/CyO* (derived from BL78781), *yw;; nos-Cas9attP2* (derived from
204 BL78782), *yw; Sp hs-hid/CyO* (derived from BL7757), *yw;; Dr hs-hid/TM3,Sb* (derived
205 from BL7758), *UAS-2xGFP* (BL6874), *wg1-17/CyO* (BL2980), *wg1-8/CyO* (BL5351),
206 *Df(2L)BSC291/CyO* (BL23676), *Mhc[k10423]/CyO* (BL10995), Df(2L)H20/CyO
207 (BL3180), *Df(2L)ED8142/SM6a* (BL24135), *hh[AC]/TM3 Sb* (BL1749),
208 *Df(3R)ED5296/TM3, Sb* (BL9338), *esgG66/CyO UAS-GFP* (BL67748),
209 *Df(2R)Exel6069/CyO* (BL7551).
210 For embryo injections, each plasmid was column purified (Qiagen) twice, eluted
211 in injection buffer (100 μM NaPO4, 5 mM KCl), and adjusted to 200ng/μl. Plasmids were
212 mixed equally by volume, and mixes were injected into *Drosophila* embryos using
213 standard procedures. For targeting genes on Chr. 2, plasmid mixes were injected into
214 *yw;; nos-Cas9attP2* embryos. For targeting genes on Chr. 3, plasmid mixes were
215 injected into *yw; nos-Cas9attP40/CyO* embryos. Approximately 500 embryos were
216 injected for each targeted gene.
217 Injected G0 flies were crossed with *yw*. We used *yw/Y hs-hid* to facilitate
218 collecting large numbers of virgin flies by incubating larvae and pupae at 37˚C for 1hr.
219 G1 flies were screened for RFP expression in the adult eye on a Zeiss Stemi SVII
220 fluorescence microscope. G1 RFP+ flies were crossed with the appropriate balancer
221 stock (*yw; Sp hs-hid/CyO* or *yw;; Dr hs-hid/TM3,Sb)*. G2 RFP+ males that were *yellow-*
222 (to remove the *nos-Cas9* transgene) and balancer+ were crossed to virgins of the
223 appropriate balancer stock (*yw; Sp hs-hid/CyO* or *yw;; Dr hs-hid/TM3,Sb*). G3 larvae

224 and pupae were heat shocked at 37˚C for 1hr to eliminate the *hs-hid* chromosome,
225 which generates a balanced stock (e.g. yw; [RFP+]/CyO).
226
227 **Imaging**
228
229 S2R+ cells expressing mNeonGreen were plated into wells of a glass-bottom 384
230 well plate (6007558, PerkinElmer). For fixed cell images, cells were incubated with 4%
231 paraformaldehyde for 30min, washed with PBS with .1% TritonX-100 (PBT) 3x 5min
232 each, stained with 1:1000 DAPI (D1306, ThermoFisher) and 1:1000 phalloidin-TRITC
233 (P1951, Sigma), and washed with PBS. Plates were imaged on an IN Cell Analyzer
234 6000 (GE) using a 20x or 60x objective. Time-lapse videos of live mNeonGreen
235 expressing single cell cloned lines were obtained by taking an image every minute using
236 a 60x objective. Images were processed using Fiji software.
237 Wing imaginal discs from 3rd instar larvae were dissected in PBS, fixed in 4%
238 paraformaldehyde, and permeabilized in PBT. For Wg staining, carcasses were blocked
239 for 1hr in 5% normal goat serum (S-1000, Vector Labs) at room temp, and incubated
240 with 1:50 mouse anti-wg (4D4, DSHB) primary antibody and 1:500 anti-mouse 488 (A-
241 21202, Molecular Probes) secondary antibody. Primary and secondary antibody
242 incubations were performed at 4˚C overnight. All carcasses were stained with DAPI and
243 phalloidin-TRITC, and mounted on glass slides with vectashield (H-1000, Vector
244 Laboratories Inc.) under a coverslip. Images of mounted wing discs were acquired on a
245 Zeiss 780 confocal microscope.
246 Larvae, pupae, and adult flies were imaged using a Zeiss Axio Zoom V16
247 fluorescence microscope.
248

249 **Quantification of mNeonGreen expressing S2R+ cells**

250

251 For FACs-based cell counting, we collected cultures from each gene knock-in
252 experiment before and after puromycin selection. Pre-selection cultures were obtained
253 by collecting of 500ul of culture 3-4 days after transfection. Post-selection cultures were
254 obtained after at least 2 weeks of puromycin incubation. Non-transfected cells were
255 used as a negative control. 100,000 cells were counted for each sample and FlowJo
256 software was used to analyze and graph the data. FSC-A vs GFP-A was plotted and we
257 defined mNeonGreen+ cells by setting a signal intensity threshold where <0.02% of
258 negative controls are counted due to autofluorescence.

259 For microscopy-based cell counting, the number of mNeonGreen cells was
260 quantified by analyzing confocal images in Fiji using the manual Cell Counter Plugin
261 (model). For transfected cells, 6 fields containing at least 200 cells were quantified (i.e.
262 n=6). For puro-selected cells, 3 fields containing at least 200 cells were quantified (i.e.
263 n=3).

264

265 **Western blotting**

266

267 Single cell-cloned cell lines were grown until confluent and 1ml of resuspended
268 cells was centrifuged at 250g for 10min. The cell pellet was resuspended in 1ml ice cold
269 PBS, re-centrifuged, and the pellet was lysed in 250ul 2x SDS-Sample buffer and boiled
270 for 5min. 10ul was loaded on a 4-20% Mini-Protean TGX SDS-Page gel (4561096,
271 BioRad), transferred to PVDF membrane (IPFL00010, Millipore), blocked in 5% non-fat
272 dry milk, primary blotting using anti-mNeonGreen (1:1000, Chromtek 32F6) or hFAB™
273 Rhodamine Anti-Actin (12004164 BioRad), and secondary blotting using 1:3000 anti-

274 mouse HRP (NXA931, Amersham), imaging using ECL (34580, ThermoFisher) on a
275 ChemiDoc MP Imaging System (BioRad).
276
277 **PCR, sequencing, and sgRNA cutting assays**
278
279 S2R+ cell genomic DNA was isolated using QuickExtract (QE09050, Lucigen).
280 Fly genomic DNA was isolated by grinding a single fly in 50µl squishing buffer (10 mM
281 Tris-Cl pH 8.2, 1 mM EDTA, 25 mM NaCl) with 200µg/ml Proteinase K (3115879001,
282 Roche), incubating at 37˚C for 30 min, and 95˚C for 2 minutes. PCR was performed
283 using Taq polymerase (TAKR001C, ClonTech) when running DNA fragments on a gel,
284 and Phusion polymerase (M-0530, NEB) was used when DNA fragments were
285 sequenced. DNA fragments corresponding to *mNeonGreen* or *T2A-Gal4* insertion sites
286 were amplified using primer pairs where one primer binds to genomic sequence and the
287 other primer binds to the insert. For amplifying non-knock-in sites, we used primers that
288 flank the sgRNA target site. Primer pairs used for gel analysis and/or Sanger
289 sequencing were designed to produce DNA fragments <1kb. Primer pairs used for next-
290 generation sequencing of the insertion site were designed to produce DNA fragments
291 200-280bp. DNA fragments were run on a 1% agarose gel for imaging or purified on
292 QIAquick columns (28115, Qiagen) for sequencing analysis. See Supplemental Table 6
293 for oligo sequences.
294 Sanger sequencing was performed at the DF/HCC DNA Resource Core facility
295 and chromatograms were analyzed using Lasergene 13 software. Next-generation
296 sequencing was performed at the MGH CCIB DNA Core. Fastq files were analyzed
297 using CRISPresso2 (CLEMENT *et al.* 2019) by entering the PCR fragment sequence into
298 the exon specification window and setting the window size to 10 bases. Quantification of

299 insertion types (seamless, in-frame in/del, and frameshift in/del) was taken from the
300 allele plot and frame shift analysis outputs of CRISPresso2. The small proportion of
301 "unmodified" reads that were not called by frameshift analysis were not included in the
302 quantification.
303 T7 endonuclease assays (M0302L, NEB) were performed following the
304 manufacturer instructions.
305
306 **Data availability:**
307
308 Donor plasmids and frame selector sgRNA plasmids will be deposited at Addgene. Fly
309 strains, S2R+ cell lines, and sequence data are available on request. Oligo and dsDNA
310 sequences are listed in Supplemental Table 6.
311
312 **Results**
313
314 To test homology-independent knock-in in *Drosophila*, we implemented a
315 strategy known as CRISPaint (SCHMID-BURGK *et al.* 2016). This system is used to insert
316 a protein tag or reporter gene into the coding sequence of an endogenous gene.
317 Although it was originally designed for mammalian cell culture, CRISPaint has several
318 advantages for use in *Drosophila*. First, this system uses CRISPR-Cas9 to induce
319 double-strand breaks (DSBs), which is known to function efficiently in *Drosophila*
320 cultured cells (BOTTCHER *et al.* 2014; VISWANATHA *et al.* 2018) and the germ line (KONDO
321 AND UEDA 2013; REN *et al.* 2013; YU *et al.* 2013; BASSETT *et al.* 2014). Second, its use of
322 a frame-selector gRNA target site makes insertion into the appropriate translation frame
323 simple and modular (see below). Third, a collection of existing CRISPaint donor

324 plasmids (SCHMID-BURGK *et al.* 2016) containing common tags (e.g. GFP, RFP,
325 Luciferase) are seemingly compatible for expression in *Drosophila*.
326 The CRISPaint system works by introducing three components into Cas9-
327 expressing cells: 1) a single guide RNA (sgRNA) targeting a genomic locus; 2) a donor
328 plasmid containing an insert sequence; and 3) a frame selector sgRNA targeting the
329 donor plasmid (Figure 1A). This causes simultaneous cleavage of the genomic locus
330 and donor plasmid, leading to the integration of linearized donor into the genomic cut
331 site by non-homologous end joining (NHEJ). To ensure that the donor plasmid inserts
332 in-frame with the endogenous gene, one of three frame selector sgRNAs are used.
333 Importantly, these frame-selector sgRNAs do not target the *Drosophila* genome.
334
335 **Homology-independent insertion functions efficiently in *Drosophila* S2R+ cells to**
336 **produce endogenous protein tags**
337
338 To test if the CRISPaint method functions in *Drosophila*, we set out to replicate
339 the findings of (SCHMID-BURGK *et al.* 2016) in cultured S2R+ cells by genetically tagging
340 endogenous proteins at their C-terminus. To accomplish this, we generated plasmids
341 expressing frame-selector sgRNAs (frame 0,1, or 2) under the control of *Drosophila* U6
342 sequences (PORT *et al.* 2015) (Figure 1A). In addition, we generated plasmids
343 expressing sgRNAs that target the 3' coding sequence of endogenous *Drosophila*
344 genes. We chose to target *Actin5c*, *His2Av*, *alphaTub84B*, and *Lamin* because these
345 genes are expressed in S2R+ cells (HU *et al.* 2017) and encode proteins with known
346 subcellular localization (actin filaments, chromatin, microtubules, nuclear envelope,
347 respectively). For donor plasmid, we used *pCRISPaint-mNeonGreen-T2A-PuroR*
348 (SCHMID-BURGK *et al.* 2016), which contains a frame-selector sgRNA target site

349 upstream of coding sequence for the fluorescent mNeonGreen protein and Puromycin
350 resistance protein (PuroR) linked by a cleavable T2A peptide sequence. Importantly,
351 only integration of the donor plasmid in-frame with the target gene coding sequence will
352 result in translation of mNeonGreen-T2A-PuroR (Figure 1A).

353 We transfected Cas9-expressing S2R+ cells (VISWANATHA *et al.* 2018) with a mix
354 of three plasmids: *pCRISPaint-mNeonGreen-T2A-PuroR* donor, target-gene sgRNA,
355 and the appropriate frame-selector sgRNA (Figure 1A, Supplemental Table 1). As an
356 initial method to detect knock-in events, we used PCR to amplify the predicted insertion
357 sites from transfected cells. Using primers that are specific to the target gene and
358 *mNeonGreen* sequence, we successfully amplified *gene-mNeonGreen* DNA fragments
359 for all four genes (Figure 1B). Furthermore, next-generation sequencing of these
360 amplified fragments revealed that 34-50% of sense-orientation insertions are in frame
361 with the target gene (Figure 1B, Supplemental Figure 1, Supplemental Table 1).

362 Next, we measured mNeonGreen fluorescence in transfected S2R+ cells as a
363 more direct method of quantifying the frequency of in-frame knock-ins. Flow cytometry-
364 based cell counting of transfected cells revealed that the number of mNeonGreen+ cells
365 range from 0.19-2.4% (Figure 1C, Supplemental Table 1), in agreement with published
366 results in human cultured cells (SCHMID-BURGK *et al.* 2016). These results were
367 confirmed by confocal analysis of transfected cells, which showed mNeonGreen
368 fluorescence in a small subset of cells (Figure 1C). Analysis of confocal images of *Act5c*
369 and *His2Av* samples showed that 3.2% and 2.4% of transfected cells expressed
370 mNeonGreen (Figure 1C, Supplemental Table 1), which roughly agreed with flow
371 cytometry cell counting. Finally, mNeonGreen localized to the expected subcellular
372 compartments, most obviously observed by His2Av-mNeonGreen and Lam-
373 mNeonGreen co-localization with the nucleus, and Act5c-mNeonGreen and alphatub-

374 mNeonGreen exclusion from the nucleus (Figure 1C). These results suggest that a
375 significant number of transfected S2R+ cells received in-frame insertion of mNeonGreen
376 at their C-terminus using the CRISPaint homology-independent insertion method.
377 For knock-in cells to be useful in experiments, it is important to derive cultures
378 where most cells, if not all, carry the insertion. Therefore, we enriched for in-frame
379 insertion events using Puromycin selection (Figure 1D). After a two-week incubation of
380 transfected S2R+ cells with Puromycin, flow-cytometry and confocal analysis revealed
381 that most cells express mNeonGreen and exhibit correct subcellular localization (Figure
382 1E, Supplemental Table 1). For *alphaTub84B*, cell counting by flow-cytometry greatly
383 underestimated the number of mNeonGreen+ cells counted by confocal analysis, likely
384 because the mNeonGreen expression level was so low. Therefore, Puromycin selection
385 is a fast and efficient method of selecting for mNeonGreen expressing knock-in cells
386 after transfection.
387 A subset of cells in Puro-selected cultures had no mNeonGreen expression or
388 unexpected localization (Figure 1E). Since each culture is composed of different cells
389 with independent insertion events, we used FACs to derive single-cell cloned lines
390 expressing mNeonGreen for further characterization (Figure 2A). At least 14 single-cell
391 cloned lines were isolated for each target gene and imaged by confocal microscopy.
392 Within a given clonal culture, every cell exhibited the same mNeonGreen localization
393 (Figure 2B), confirming our single-cell cloning approach and demonstrating that the
394 insertion is genetically stable over many cell divisions. Importantly, while many clones
395 exhibited the predicted mNeonGreen localization, a subset of the clonal cell lines
396 displayed an unusual localization pattern (Figure 2B). For example, three *Act5c-*
397 *mNeonGreen* clones had localization in prominent rod structures, and 12 *Lamin-*
398 *mNeonGreen* clones had asymmetric localization in the nuclear envelope (Figure 2B).

399 In addition, some clones had diffuse mNeonGreen localization in the cytoplasm and
400 nucleus (Figure 2B).

401 To better characterize the insertions in single cell-cloned lines, we further
402 analyzed three clones per gene (12 total), selecting different classes when possible
403 (correct localization, unusual localization, and diffuse localization) (Supplemental Table
404 2). Using PCR amplification of the predicted insertion site (Figure 1A, Figure 2C) and
405 sequencing of amplified fragments (Supplemental Table 2), we determined that all
406 clones with correct or unusual mNeonGreen localization contained an in-frame insertion
407 of mNeonGreen with the target gene. In contrast, we were unable to amplify DNA
408 fragments from the expected insertion site in clones with diffuse mNeonGreen
409 localization (Figure 2C). Western blotting of cell lysates confirmed that only clones with
410 in-frame mNeonGreen insertion express fusion proteins that match the predicted
411 molecular weights (Figure 2D). All together, these results suggest that clones with
412 correct mNeonGreen localization are likely to contain an in-frame insert in the correct
413 target gene.

414 Since S2R+ cells are polyploid (LEE *et al.* 2014), clones expressing mNeonGreen
415 could bear one or more insertions. Furthermore, in/dels induced at the non-insertion
416 locus could disrupt protein function. To explore these possibilities, we amplified the non-
417 insertion locus in our single-cell cloned lines and used Sanger and next-generation
418 sequencing to analyze the DNA fragments (Figure 2C, Supplemental Table 2). For each
419 gene, we could find in/dels occurring at the non-insertion sgRNA cut site. For example,
420 we could distinguish four distinct alleles in clone B11: a 3bp deletion, a 2bp deletion, a
421 1bp deletion, and a 27bp deletion. In addition, we identified an unusual mutation in
422 clone C6, where a 1482bp DNA fragment inserted at the sgRNA cut site, which
423 corresponds to a region from *alphatub84D*. We assume that this large insertion was

424 caused by homologous recombination, since *alphatub84D* and *alphatub84B* share 92%
425 genomic sequence identity (Flybase). For *Act5c-mNeonGreen* clones A5 and A19,
426 numerous in/del sequences were found, suggesting this region has an abnormal
427 number of gene copies. We were unable to amplify a DNA fragment from *Lam-*
428 *mNeonGreen* D9, despite follow-up PCRs using primers that bind genomic sequence
429 further away from the insertion site (not shown).
430 One useful application of cell lines with fluorescently tagged endogenous
431 proteins is to track their localization over time. Therefore, we used live confocal imaging
432 of our single-cell cloned lines to capture mNeonGreen localization during cell division
433 (Figure 2E, Supplemental Videos). Time-lapse images of dividing cells showed that
434 Act5c-mNeonGreen localized to rod structures that asymmetrically or symmetrically
435 distribute into daughter cells, His2Av-mNeonGreen localized to chromosomes that
436 segregate into daughter cells, Lam-mNeonGreen showed disassembly and reassembly
437 at the nuclear envelope, and alphaTub84B-mNeonGreen localized to mitotic spindles.
438 These results demonstrate the usefulness of knock-in *Drosophila* cell lines to track the
439 dynamic localization of endogenous proteins.
440

441 ***In vivo* germ line knock-in of T2A-Gal4 into endogenous genes using homology-**
442 **independent insertion**
443

444 We next tested if homology-independent insertion could function in the
445 *Drosophila* germ line for the purpose of generating knock-in fly strains. Compared to
446 cultured cells, the isolation of flies bearing insertions that are in-frame with endogenous
447 genes required additional considerations. As opposed to antibiotic selection, visible
448 markers are commonly used to identify transgenic animals. In addition, since some

449 genes are expressed at low levels, target gene expression of an inserted reporter
450 element may be insufficient to identify in-frame insertion events.
451 To overcome these issues, we constructed the donor plasmid *pCRISPaint-T2A-*
452 *Gal4-3xP3-RFP* (Figure 3A). This donor contains a frame-selector sgRNA target site
453 upstream of the reporter gene *T2A-Gal4*, which encodes a form of the transcription
454 factor Gal4 that is cleaved from tagged endogenous protein (DIAO AND WHITE 2012).
455 Insertion of this element in-frame with genomic coding sequence would result in Gal4
456 translation, which can be detected using a *UAS-reporter* transgene (BRAND AND
457 PERRIMON 1993). In addition, this donor plasmid contains a *3xP3-RFP* selectable marker
458 gene that expresses bright red fluorescence in *Drosophila* larval tissues and the adult
459 eye (BERGHAMMER *et al.* 1999; GRATZ *et al.* 2014) (Figure 3B). Importantly, the
460 expression of *3xP3-RFP* is not dependent on in-frame insertion with the target gene.
461 Next, we tested for *pCRISPaint-T2A-Gal4-3xP3-RFP* insertion into 11
462 endogenous genes (Supplemental Table 3). These genes were selected based on their
463 known expression pattern, expression levels, or loss of function phenotype.
464 Furthermore, we targeted *pCRISPaint-T2A-Gal4-3xP3-RFP* to insert into the 5' portion
465 of the coding sequence (Figure 3A). This insertion location is designed to disrupt the
466 protein product by premature truncation. Plasmid mixes were injected into *nos-Cas9*
467 embryos, the resulting G0 progeny were outcrossed to *yw*, and G1 adults were
468 screened for RFP fluorescence (Figure 3C). Each RFP+ founder fly was outcrossed to
469 an appropriate balancer stock to establish a stable line. Figure 3D and Supplemental
470 Table 3 shows the integration efficiency results for each gene and Supplemental Table
471 4 has information on each balanced RFP+ line. From this data, we find that the
472 frequency of G0 crosses yielding RFP+ G1 progeny varies between 5% and 21%
473 (Figure 3D, Supplemental Table 3). For example, when targeting *ebony* with *pFP545*, 3

474 out of 16 G0 crosses produced ≥1 RFP+ G1 flies. Therefore, the *pCRISPaint-T2A-Gal4-*
475 *3xP3-RFP* donor can insert into the genome of germ line cells in a homology-
476 independent manner.

477 To gain insight into the genomic location of the insertions in our RFP+ lines, we
478 first analyzed them by simple genetic crosses. During the fly stock balancing process,
479 we determined that each insertion was located on the intended chromosome
480 (Supplemental Table 4). In addition, flies that were homozygous for the insertion
481 exhibited known phenotypes. For example, homozygous insertions in *ebony* produced
482 flies with dark cuticle pigment (Figure 3E). Furthermore, flies with insertions targeting
483 *wg*, *Mhc*, *hh*, and *esg* were homozygous lethal, which is consistent with known loss of
484 function mutations in these genes (Supplemental Table 4). To test if the lethality of flies
485 with homozygous insertions was due to on- or off-target gene disruption, we performed
486 complementation tests by crossing RFP+ insertion lines with lines containing a known
487 loss of function allele or genomic deletion spanning the gene. In all cases tested, trans-
488 heterozygous combinations were lethal (Supplemental Table 4). Together, these results
489 suggest that the *pCRISPaint-T2A-Gal4-3xP3-RFP* donor plasmid inserted into the
490 intended target genes.

491 For T2A-Gal4 to be expressed by the target gene, the linearized donor plasmid
492 must insert in the sense orientation relative to the target gene and in-frame with the
493 coding sequence. As an initial screen for such events, we crossed RFP+ lines to a *UAS-*
494 *GFP* line and assayed progeny for fluorescence. Through this approach, we identified
495 Gal4-expressing lines for *ebony*, *myo1a*, *wg*, and *Mhc* (Figure 4A, Supplemental Tables
496 3, 4). *wg-T2A-Gal4* (#1 and 4), *Mhc-T2A-Gal4* (#1 and 2), and *Myo1a-T2A-Gal4* (#1)
497 insertions express in the imaginal disc, larval muscle, and larval gut (Figure 4A),
498 respectively, which matches the known expression patterns for these genes.

499 Furthermore, *wg-T2A-Gal4 #1 and #4* insertions were expressed in a distinctive Wg
500 pattern in the wing disc pouch (Figure 4B). The expression pattern of *ebony* is less well
501 understood. We find that *ebony-T2A-Gal4 pFP545 #2* is expressed in the larval brain
502 (Figure 4A) and throughout the pupal body (Figure 4C), which is consistent with a
503 previous study (HOVEMANN *et al.* 1998). However, *ebony-T2A-Gal4 pFP545 #2* is also
504 expressed in the larval tracheal openings (Figure 4A), indicating that *ebony* may play a
505 role in this tissue.

506 Next, we analyzed the insertion orientation and sequence structure in the RFP+
507 lines that express Gal4. We PCR amplified a region flanking the predicted insertion site
508 from genomic DNA using primer pairs to distinguish sense and anti-sense insertions
509 (Supplemental Figure 2). All RFP+ lines with Gal4 expression had insertions that were
510 in the sense orientation (Supplemental Table 4, Supplemental Figure 2). Sequencing
511 the resulting PCR fragments showed that the insert was present at the sgRNA cut site
512 and each insertion contained an in/del between the target gene and *T2A-Gal4*
513 sequence (Figure 4D). For example, *ebony-T2A-Gal4 pFP545 #2* contains a 15bp
514 genomic deletion that is predicted to keep T2A-Gal4 in-frame with ebony. Similarly, *wg-*
515 *T2A-Gal4* #1 contains an in-frame 45bp deletion and 21bp insertion. Remarkably, *wg-*
516 *T2A-Gal4* #4 contains a frameshift in/del (Figure 4D), yet still expresses Gal4 in the Wg
517 pattern, albeit at significantly lower levels than *wg-T2A-Gal4* #1 (Figure 4B). In similar
518 cases, *Mhc-T2A-Gal4* lines #1, #2, and *Myo1a-T2A-Gal4* #1, each have in/dels that put
519 *T2A-Gal4* out of frame with the target gene coding sequence. These findings confirm
520 that our Gal4-expressing lines have *T2A-Gal4* inserted in the correct gene and
521 orientation, but that in-frame insertion with the target gene is not necessarily a
522 requirement.

523 To better characterize the insertion events in our collection of RFP+ lines, we
524 analyzed those that did not produce fluorescence when crossed with *UAS-GFP*
525 (Supplemental Table 4, Supplemental Figures 2,3). Using PCR and sequencing
526 analysis, we found that some lines contained insertions in the correct target site but in
527 the anti-sense orientation. In addition, we identified lines with insertions in the sense
528 orientation, but were out of frame relative to the target gene. Unexpectedly, we found
529 that *wg-T2A-Gal4* #6 contained a sense orientation in-frame insertion. Yet, unlike *wg-*
530 *T2A-Gal4* #1, *wg-T2A-Gal4* #6 does not express Gal4. Importantly, our molecular
531 analysis of every independently isolated RFP+ line (20 in total) revealed that each
532 contained an insertion in the intended target site (Supplemental Table 4, Supplemental
533 Figures 2,3).
534 We did not obtain RFP+ insertions when targeting *ap*, *alphaTub84B*, *btl*, or
535 *Desat1*. Therefore, we investigated whether the sgRNAs targeting these genes were
536 functional. All 4 sgRNAs used for germ line knock-ins have an acceptable efficiency
537 score of >5, with the exception of the sgRNA targeting *btl* (Supplemental Table 5). We
538 tested whether the sgRNAs were functional in transfected S2R+ cells by performing a
539 T7 endonuclease assay that detects in/dels at the cut site. This test revealed that
540 sgRNAs targeting *ap*, *alphaTub84B*, *btl* can cut at the target site, whereas the results
541 with *desat1* were inconclusive (Supplemental Figure 4A). As an alternative functional
542 test, we used PCR to detect knock-in events in S2R+ cells transfected with the
543 *pCRISPaint-T2A-Gal4-3xP3-RFP* donor plasmid. This showed that sgRNAs targeting
544 *ap*, *alphaTub84B*, *btl* and *desat1* can successfully knock-in *pCRISPaint-T2A-Gal4-*
545 *3xP3-RFP* (Supplemental Figure 4B). Finally, we sequenced the sgRNA target sites in
546 the *nos-Cas9* fly strains and found a SNP in the *btl* sgRNA binding site (not shown). The
547 10 remaining sgRNAs had no SNPs in the target site. In summary, we conclude that the

548 sgRNAs targeting *ap*, *alphaTub84B*, *btl*, and *Desat1* are able to induce cleavage at their
549 target site in S2R+ cells, but that the sgRNA targeting *btl* will not function in the germ
550 line using our *nos-Cas9* strains.
551
552 **A resource of CRISPaint donor plasmids for germ line knock-ins in Drosophila**
553
554 To facilitate the insertion of other sequences using the CRISPaint insertion
555 method, we generated 10 additional donor plasmids based on the same architecture as
556 *pCRISPaint-T2A-Gal4-3xP3-RFP* (Figure 5A). These include T2A-containing donors
557 with sequence encoding the alternative binary reporters LexGAD, QF2, and split-Gal4,
558 as well as Cas9 nuclease, FLP recombinase, Gal80 repression protein, NanoLuc
559 luminescence reporter, and super-folder GFP. Like *T2A-Gal4*, these can be used to
560 insert at 5' coding sequence, capturing endogenous gene expression and generating a
561 loss-of function. In addition, we generated *pCRISPaint-sfGFP-3xP3-RFP*, which can be
562 used to insert into 3' coding sequence, generating a C-terminal GFP fusion protein.
563 Several groups have demonstrated that coding sequence containing a splice
564 acceptor (SA) and inserted in a gene intron can produce a protein trap with the
565 preceding coding exon (Morin *et al.* 2001; Venken *et al.* 2011). Recently, two studies
566 produced *SA-T2A-Gal4* donor plasmids for intron insertion by HDR, called CRIMIC and
567 T-GEM (Diao *et al.* 2015; Lee *et al.* 2018). Therefore, we modified these two plasmids to
568 contain a CRISPaint target site upstream of the splice acceptor (Figure 5B).
569
570 **Discussion**
571

572 The insertion of large DNA elements into the genome by HDR requires a great
573 deal of expertise and labor for the design and construction of donor plasmids. Some
574 groups have developed strategies to improve the efficiency and scale at which
575 homology arms are cloned into donor plasmids (HOUSDEN *et al.* 2014; GRATZ *et al.*
576 2015), but the root problem still remains. Furthermore, each new gene-specific donor
577 plasmid requires the same amount of investment for their construction but is only used
578 once to achieve the desired knock-in. For these reasons, we believe that the current
579 methods for knock-in by HDR may act as a barrier to achieving widespread use by the
580 *Drosophila* community.

581 In this study, we addressed these challenges by demonstrating that large DNA
582 elements can insert into the *Drosophila* genome by a homology-independent
583 mechanism, using the previously established CRISPaint system. This approach has two
584 major advantages over HDR. 1) No construction of a donor plasmid is necessary, as
585 long as a suitable CRISPaint-compatible donor plasmid already exists. The only unique
586 reagent needed is an sgRNA that targets the endogenous gene (also required for HDR).
587 Cloning sgRNAs into expression plasmids, such as *pCFD3* (PORT *et al.* 2014), is simple,
588 fast, inexpensive, and works nearly every time. Furthermore, the availability of sgRNA-
589 encoding plasmids from public resources (e.g. TRiP, Addgene), and synthesized
590 sgRNA from commercial companies, means that researchers can increasingly order
591 their sgRNAs. 2) CRISPaint-compatible donor plasmids are “universal” and thus
592 modular. For example, different genes can be targeted by the same CRISPaint donor
593 plasmid, and different CRISPaint donor plasmids can be targeted to the same gene.
594 Publicly available collections of CRISPaint donor plasmids [(SCHMID-BURGK *et al.* 2016),
595 this study] ensure that researchers only need to select their insert of choice. Indeed, the
596 CRISPaint donor plasmids originally used for mammalian cell culture also function in

597 *Drosophila* S2R+ cells (Figure 1) and the *3xP3-RFP* marker in our germ line donor
598 plasmids is compatible with other insects (BERGHAMMER *et al.* 1999).
599 An important step in obtaining correctly targeted knock-ins is molecularly
600 validating the candidate insertions. Confirming an HDR insertion requires amplifying a
601 large DNA fragment (~1.5kb-2kb) that encompasses part of the insert, an entire
602 homology arm, and a portion of genomic sequence flanking the homology arm. This is
603 necessary to verify that the donor did not insert off-target. These PCRs can sometimes
604 fail or give inconclusive results due to the large fragment size. In contrast, CRISPaint
605 knock-ins are easier to characterize by PCR analysis and sequencing because the
606 amplified region is relatively small (~200-800bp) (Figure 1B, Figure 2C, Supplemental
607 Figures 2,4). However, CRISPaint knock-ins require more work to screen since they can
608 insert in two directions and in/dels occur at the insertion site. When possible, we
609 recommend that researchers select for insert expression before molecular validation.
610 In this study, we generated knock-ins by inserting the entire linearized CRISPaint
611 donor plasmid into the target gene. Since the backbone contains bacterial sequences, it
612 may cause transgene silencing or impact neighboring gene expression (CHEN *et al.*
613 2004; SUZUKI *et al.* 2016). However, we note that thousands of transgenic fly lines
614 contain bacterial sequences from phiC31 integration (PERKINS *et al.* 2015) with no
615 reports of ill effects. Another issue is that insertion of the entire plasmid restricts the
616 design of gene-tagging events to only append the insert 3' to the target insertion site.
617 Different groups have used approaches that address these issues, such as providing
618 donor plasmids as mini-circles (SCHMID-BURGK *et al.* 2016; SUZUKI *et al.* 2016), cutting
619 donor plasmid twice to liberate the insert fragment (LACKNER *et al.* 2015; SUZUKI *et al.*
620 2016), or using PCR amplified inserts (Manna et al. 2019 BioRxiv). The first two
621 modifications could in theory be made to our germ-line donor plasmids (e.g.

622 *pCRISPaint-T2A-Gal4-3xP3-RFP*), but for this study we opted to establish the simplest
623 protocol possible. Furthermore, we reasoned that cutting the donor twice would give rise
624 to two donor fragments and this could reduce knock-in efficiency.

625 Using the CRISPaint method in S2R+ cells, we readily identified cell lines with
626 endogenous proteins tagged with mNeonGreen at their C-terminus (Figure 2,
627 Supplemental Table 2). However, some lines exhibited unusual or unexpected protein
628 localization. In clones D6 and D9, Lamin-mNeonGreen localizes to the nuclear
629 envelope, but in D9 this localization is enriched asymmetrically in the direction of the
630 previous plane of cell division. Since these two clones contain the same seamless
631 mNeonGreen insertion, we speculate that mutations at non-knock-in loci account for this
632 difference. Indeed, clone D6 contained an in-frame 3bp deletion at the non-knock-in
633 locus, likely retaining wild-type function, whereas D9 had no remaining non-knock-in
634 locus. We saw a similar pattern for clones A3 and A5, where both had seamless
635 mNeonGreen insertions in *Actin5c*, but clone A5 exhibited distinct rod structures.
636 Finally, alphaTub84B-mNeonGreen fluorescence and protein levels were extremely low
637 in all cell lines, despite *alphaTub84B* being highly expressed in S2R+ cells (HU *et al.*
638 2017). We speculate that the alphaTub84B-mNeonGreen fusion protein is unstable and
639 previous studies in other organisms have highlighted problems with C-terminal tagging
640 of alpha-Tubulin (CARMINATI AND STEARNS 1997). Similarly, C-terminal tags can disrupt
641 Lamin and Actin function (DAVIES *et al.* 2009; NAGASAKI *et al.* 2017). These findings
642 illustrate the need for experimenters to consider the existing knowledge of the protein
643 when generating C-terminal protein fusions, and to carefully screen individual single cell
644 cloned lines.

645 We constructed a CRISPaint-compatible *T2A-Gal4* donor plasmid for use in the
646 fly germ line and successfully identified insertion lines. Our knock-in efficiency, defined
647 by the percentage of injected G0 flies that give RFP+ progeny, ranged from 5-21%
648 (Figure 3B, Supplemental Table 3), which is roughly similar to knock-in efficiencies
649 observed when using HDR [5-22% (GRATZ *et al.* 2014), 46-88% (PORT *et al.* 2015), 7-
650 42% (GRATZ *et al.* 2015)]. In addition, all 20 of our RFP+ fly lines, which encompass 8
651 different sgRNA target sites, contain an insertion at the correct location. Though, we do
652 not rule out the possibility of a second-site off-target event on the same chromosome.
653 To obtain *T2A-Gal4* insertions that express Gal4 under the control of the target
654 gene (Figure 4), it was necessary to screen multiple independently derived insertions,
655 due to the in/dels that occur at the insertion site and the two insertion orientations.
656 However, we found for some genes the overall efficiencies were too low to obtain a
657 successful Gal4-expressing line (*hh*, *esg, FK506-bp2*), or we did not obtain any RFP+
658 insertions (*ap*, *alphaTub84B*, *btl*, and *Desat1*). Additional steps could be taken to
659 improve insertion efficiency, such as optimization of the injected plasmid concentrations,
660 increasing the number of injected embryos, or simply reattempting with a different
661 sgRNA. It is also possible that certain insertions are toxic to cells/animals during G0
662 germ-line development or in G1 progeny.
663 There were three unexpected findings with our germ-line insertions. First, some
664 Gal4-expressing lines had *T2A-Gal4* inserted out of frame relative to the target gene.
665 We speculate that it may be the result of ribosome frameshifting (KETTELER 2012), an
666 internal ribosome entry site (IRES) (KOMAR AND HATZOGLOU 2005), or the presence of
667 alternative open reading frames (altORFs) (MOUILLERON *et al.* 2016). However, we find
668 no obvious evidence of these mechanisms by analyzing the sequence flanking *wg*, *Mhc*,
669 and *Myo1a* insertion sites (not shown). Ultimately, we consider this a fortuitous effect as

670 long as Gal4 is expressed in the correct pattern. Second, we found an in-frame insertion
671 in *wg* (#6) that that does not express Gal4. This finding highlights the importance of
672 screening RFP+ insertions for Gal4 expression when possible. Third, we found that,
673 unlike in cell culture, all of our RFP+ fly lines contain in/dels at the insertion site. Germ
674 cells are known to differ in their NHEJ mechanisms compared to somatic cells (PRESTON
675 *et al.* 2006; AHMED *et al.* 2015), but it is not clear why this would reduce the frequency of
676 seamless insertions. Perhaps genetic or chemical manipulation of NHEJ regulators
677 during embryo injection could address this issue in the future. This finding also suggests
678 that the CRISPaint frame-selector approach may not be as useful in the fly germ line as
679 it is in cell culture.

680 Our collection of donor plasmids (Figure 5) provides many options for inserting
681 protein-coding sequence into target genes. However, other uses for homology-
682 independent knock-in can be imagined, such as inserting enhancer sequences (e.g.
683 *UAS*) upstream of endogenous genes to induce their overexpression (RORTH 1996), a
684 reporter gene near non-coding regulatory sequences to capture the transcriptional
685 expression pattern of neighboring genes (BRAND AND PERRIMON 1993), entire genes into
686 intergenic sequence (SADELAIN *et al.* 2011), or sequences to be used for labeling DNA
687 loci (ROBINETT *et al.* 1996). Furthermore, the donor plasmids described in this study
688 could be used to simply knock out endogenous genes with a selectable marker. Indeed,
689 all of our mNeonGreen-expressing single cell cloned lines contain mutations in the non-
690 knock-in locus and our fly germ line insertions produced loss of function phenotypes.
691 This approach could greatly increase the efficiency of selecting knock-out alleles, which
692 are traditionally done by laborious PCR-based screening of frameshift in/dels. We also
693 note that, similar to the *T2A-Gal4* reporters in vivo, cell lines could be targeted with
694 translational reporters such as NanoLuciferase or GFP. Finally, since our collection of

695 CRISPaint donor plasmids contain enzyme restriction sites that flank the insert
696 sequence, they are also useful as parental vectors for constructing traditional HDR
697 donor plasmids.
698 In summary, our homology-independent knock-in approach enables researchers
699 to focus more effort on screening for correct insertions in cells or flies than on designing
700 and constructing donor plasmids. Furthermore, the techniques required for screening
701 knock-ins are less specialized than those for constructing donor plasmids, making this
702 trade off potentially attractive for labs with less molecular biology expertise or resources.
703 Therefore, we hope that this method will put knock-in technology into the hands of more
704 researchers due to its simplicity.
705
706 **Acknowledgements**
707
708 We thank Jonathan Schmid-Burgk for advice and the *CRISPaint-mNeonGreen* donor
709 plasmid, Claire Hu and the TRiP for sgRNA design and construction, Ben Ewen-
710 Campen for valuable comments on the manuscript, Stephanie Mohr, Oguz Kanca, and
711 Hugo Bellen for helpful discussions, Raghuvir Viswanatha for the *Cas9-T2A-EGFP*
712 template sequence, and Rich Binari and Cathryn Murphy for general assistance. J.A.B.
713 was supported by the Damon Runyon Foundation. This work was supported by NIH
714 grants R01GM084947, R01GM067761, R24OD019847. N.P. is an investigator of the
715 Howard Hughes Medical Institute.
716
717 **References:**
718

719 Ahmed, E. A., H. Scherthan and D. G. de Rooij, 2015 DNA Double Strand Break
720 Response and Limited Repair Capacity in Mouse Elongated Spermatids. Int J
721 Mol Sci 16: 29923-29935.
722 Auer, T. O., K. Duroure, A. De Cian, J. P. Concordet and F. Del Bene, 2014 Highly
723 efficient CRISPR/Cas9-mediated knock-in in zebrafish by homology-independent
724 DNA repair. Genome Res 24: 142-153.
725 Bassett, A. R., C. Tibbit, C. P. Ponting and J. L. Liu, 2014 Mutagenesis and homologous
726 recombination in Drosophila cell lines using CRISPR/Cas9. Biol Open 3: 42-49.
727 Bellen, H. J., R. W. Levis, Y. He, J. W. Carlson, M. Evans-Holm *et al.*, 2011 The
728 Drosophila gene disruption project: progress using transposons with distinctive
729 site specificities. Genetics 188: 731-743.
730 Berghammer, A. J., M. Klingler and E. A. Wimmer, 1999 A universal marker for
731 transgenic insects. Nature 402: 370-371.
732 Bier, E., M. M. Harrison, K. M. O'Connor-Giles and J. Wildonger, 2018 Advances in
733 Engineering the Fly Genome with the CRISPR-Cas System. Genetics 208: 1-18.
734 Bosch, J. A., N. H. Tran and I. K. Hariharan, 2015 CoinFLP: a system for efficient
735 mosaic screening and for visualizing clonal boundaries in Drosophila.
736 Development 142: 597-606.
737 Bottcher, R., M. Hollmann, K. Merk, V. Nitschko, C. Obermaier *et al.*, 2014 Efficient
738 chromosomal gene modification with CRISPR/cas9 and PCR-based homologous
739 recombination donors in cultured Drosophila cells. Nucleic Acids Res 42: e89.
740 Bouabe, H., and K. Okkenhaug, 2013 Gene targeting in mice: a review. Methods Mol
741 Biol 1064: 315-336.
742 Brand, A. H., and N. Perrimon, 1993 Targeted gene expression as a means of altering
743 cell fates and generating dominant phenotypes. Development 118: 401-415.
744 Carminati, J. L., and T. Stearns, 1997 Microtubules orient the mitotic spindle in yeast
745 through dynein-dependent interactions with the cell cortex. J Cell Biol 138: 629-
746 641.
747 Chen, Z. Y., C. Y. He, L. Meuse and M. A. Kay, 2004 Silencing of episomal transgene
748 expression by plasmid bacterial DNA elements in vivo. Gene Ther 11: 856-864.
749 Clement, K., H. Rees, M. C. Canver, J. M. Gehrke, R. Farouni *et al.*, 2019
750 CRISPResso2 provides accurate and rapid genome editing sequence analysis.
751 Nat Biotechnol 37: 224-226.
752 Cristea, S., Y. Freyvert, Y. Santiago, M. C. Holmes, F. D. Urnov *et al.*, 2013 In vivo
753 cleavage of transgene donors promotes nuclease-mediated targeted integration.
754 Biotechnol Bioeng 110: 871-880.
755 Crivat, G., and J. W. Taraska, 2012 Imaging proteins inside cells with fluorescent tags.
756 Trends Biotechnol 30: 8-16.
757 Davies, B. S., L. G. Fong, S. H. Yang, C. Coffinier and S. G. Young, 2009 The
758 posttranslational processing of prelamin A and disease. Annu Rev Genomics
759 Hum Genet 10: 153-174.
760 Diao, F., H. Ironfield, H. Luan, F. Diao, W. C. Shropshire *et al.*, 2015 Plug-and-play
761 genetic access to drosophila cell types using exchangeable exon cassettes. Cell
762 Rep 10: 1410-1421.
763 Diao, F., and B. H. White, 2012 A novel approach for directing transgene expression in
764 Drosophila: T2A-Gal4 in-frame fusion. Genetics 190: 1139-1144.
765 Gratz, S. J., C. D. Rubinstein, M. M. Harrison, J. Wildonger and K. M. O'Connor-Giles,
766 2015 CRISPR-Cas9 Genome Editing in Drosophila. Curr Protoc Mol Biol 111: 31
767 32 31-20.

768 Gratz, S. J., F. P. Ukken, C. D. Rubinstein, G. Thiede, L. K. Donohue *et al.*, 2014 Highly
769 specific and efficient CRISPR/Cas9-catalyzed homology-directed repair in
770 Drosophila. Genetics 196**:** 961-971.
771 Hasse, S., A. A. Hyman and M. Sarov, 2016 TransgeneOmics--A transgenic platform for
772 protein localization based function exploration. Methods 96**:** 69-74.
773 Housden, B. E., S. Lin and N. Perrimon, 2014 Cas9-based genome editing in
774 Drosophila. Methods Enzymol 546**:** 415-439.
775 Housden, B. E., M. Muhar, M. Gemberling, C. A. Gersbach, D. Y. Stainier *et al.*, 2017
776 Loss-of-function genetic tools for animal models: cross-species and cross-
777 platform differences. Nat Rev Genet 18**:** 24-40.
778 Hovemann, B. T., R. P. Ryseck, U. Walldorf, K. F. Stortkuhl, I. D. Dietzel *et al.*, 1998
779 The Drosophila ebony gene is closely related to microbial peptide synthetases
780 and shows specific cuticle and nervous system expression. Gene 221**:** 1-9.
781 Hu, Y., A. Comjean, N. Perrimon and S. E. Mohr, 2017 The Drosophila Gene
782 Expression Tool (DGET) for expression analyses. BMC Bioinformatics 18**:** 98.
783 Ivics, Z., M. A. Li, L. Mates, J. D. Boeke, A. Nagy *et al.*, 2009 Transposon-mediated
784 genome manipulation in vertebrates. Nat Methods 6**:** 415-422.
785 Kanca, O., H. J. Bellen and F. Schnorrer, 2017 Gene Tagging Strategies To Assess
786 Protein Expression, Localization, and Function in Drosophila. Genetics 207**:** 389-
787 412.
788 Katic, I., L. Xu and R. Ciosk, 2015 CRISPR/Cas9 Genome Editing in Caenorhabditis
789 elegans: Evaluation of Templates for Homology-Mediated Repair and Knock-Ins
790 by Homology-Independent DNA Repair. G3 (Bethesda) 5**:** 1649-1656.
791 Katoh, Y., S. Michisaka, S. Nozaki, T. Funabashi, T. Hirano *et al.*, 2017 Practical
792 method for targeted disruption of cilia-related genes by using CRISPR/Cas9-
793 mediated, homology-independent knock-in system. Mol Biol Cell 28**:** 898-906.
794 Ketteler, R., 2012 On programmed ribosomal frameshifting: the alternative proteomes.
795 Front Genet 3**:** 242.
796 Kimple, M. E., A. L. Brill and R. L. Pasker, 2013 Overview of affinity tags for protein
797 purification. Curr Protoc Protein Sci 73**:** Unit 9 9.
798 Komar, A. A., and M. Hatzoglou, 2005 Internal ribosome entry sites in cellular mRNAs:
799 mystery of their existence. J Biol Chem 280**:** 23425-23428.
800 Kondo, S., and R. Ueda, 2013 Highly improved gene targeting by germline-specific
801 Cas9 expression in Drosophila. Genetics 195**:** 715-721.
802 Korona, D., S. A. Koestler and S. Russell, 2017 Engineering the Drosophila Genome for
803 Developmental Biology. J Dev Biol 5.
804 Lackner, D. H., A. Carre, P. M. Guzzardo, C. Banning, R. Mangena *et al.*, 2015 A
805 generic strategy for CRISPR-Cas9-mediated gene tagging. Nat Commun 6**:**
806 10237.
807 Lee, H., C. J. McManus, D. Y. Cho, M. Eaton, F. Renda *et al.*, 2014 DNA copy number
808 evolution in Drosophila cell lines. Genome Biol 15**:** R70.
809 Lee, P. T., J. Zirin, O. Kanca, W. W. Lin, K. L. Schulze *et al.*, 2018 A gene-specific T2A-
810 GAL4 library for Drosophila. Elife 7.
811 Maresca, M., V. G. Lin, N. Guo and Y. Yang, 2013 Obligate ligation-gated
812 recombination (ObLiGaRe): custom-designed nuclease-mediated targeted
813 integration through nonhomologous end joining. Genome Res 23**:** 539-546.
814 Morin, X., R. Daneman, M. Zavortink and W. Chia, 2001 A protein trap strategy to
815 detect GFP-tagged proteins expressed from their endogenous loci in Drosophila.
816 Proc Natl Acad Sci U S A 98**:** 15050-15055.

817 Mouilleron, H., V. Delcourt and X. Roucou, 2016 Death of a dogma: eukaryotic mRNAs
818 can code for more than one protein. Nucleic Acids Res 44**:** 14-23.
819 Nagasaki, A., T. K. S, T. Yumoto, M. Imaizumi, A. Yamagishi *et al.*, 2017 The Position
820 of the GFP Tag on Actin Affects the Filament Formation in Mammalian Cells. Cell
821 Struct Funct 42**:** 131-140.
822 Perkins, L. A., L. Holderbaum, R. Tao, Y. Hu, R. Sopko *et al.*, 2015 The Transgenic
823 RNAi Project at Harvard Medical School: Resources and Validation. Genetics
824 201**:** 843-852.
825 Port, F., H. M. Chen, T. Lee and S. L. Bullock, 2014 Optimized CRISPR/Cas tools for
826 efficient germline and somatic genome engineering in Drosophila. Proc Natl Acad
827 Sci U S A 111**:** E2967-2976.
828 Port, F., N. Muschalik and S. L. Bullock, 2015 Systematic Evaluation of Drosophila
829 CRISPR Tools Reveals Safe and Robust Alternatives to Autonomous Gene
830 Drives in Basic Research. G3 (Bethesda) 5**:** 1493-1502.
831 Preston, C. R., C. C. Flores and W. R. Engels, 2006 Differential usage of alternative
832 pathways of double-strand break repair in Drosophila. Genetics 172**:** 1055-1068.
833 Quadros, R. M., H. Miura, D. W. Harms, H. Akatsuka, T. Sato *et al.*, 2017 Easi-CRISPR:
834 a robust method for one-step generation of mice carrying conditional and
835 insertion alleles using long ssDNA donors and CRISPR ribonucleoproteins.
836 Genome Biol 18**:** 92.
837 Ren, X., J. Sun, B. E. Housden, Y. Hu, C. Roesel *et al.*, 2013 Optimized gene editing
838 technology for Drosophila melanogaster using germ line-specific Cas9. Proc Natl
839 Acad Sci U S A 110**:** 19012-19017.
840 Robinett, C. C., A. Straight, G. Li, C. Willhelm, G. Sudlow *et al.*, 1996 In vivo localization
841 of DNA sequences and visualization of large-scale chromatin organization using
842 lac operator/repressor recognition. J Cell Biol 135**:** 1685-1700.
843 Rorth, P., 1996 A modular misexpression screen in Drosophila detecting tissue-specific
844 phenotypes. Proc Natl Acad Sci U S A 93**:** 12418-12422.
845 Sadelain, M., E. P. Papapetrou and F. D. Bushman, 2011 Safe harbours for the
846 integration of new DNA in the human genome. Nat Rev Cancer 12**:** 51-58.
847 Schmid-Burgk, J. L., K. Honing, T. S. Ebert and V. Hornung, 2016 CRISPaint allows
848 modular base-specific gene tagging using a ligase-4-dependent mechanism. Nat
849 Commun 7**:** 12338.
850 Suzuki, K., Y. Tsunekawa, R. Hernandez-Benitez, J. Wu, J. Zhu *et al.*, 2016 In vivo
851 genome editing via CRISPR/Cas9 mediated homology-independent targeted
852 integration. Nature 540**:** 144-149.
853 Venken, K. J., A. Sarrion-Perdigones, P. J. Vandeventer, N. S. Abel, A. E. Christiansen
854 *et al.*, 2016 Genome engineering: Drosophila melanogaster and beyond. Wiley
855 Interdiscip Rev Dev Biol 5**:** 233-267.
856 Venken, K. J., K. L. Schulze, N. A. Haelterman, H. Pan, Y. He *et al.*, 2011 MiMIC: a
857 highly versatile transposon insertion resource for engineering Drosophila
858 melanogaster genes. Nat Methods 8**:** 737-743.
859 Viswanatha, R., Z. Li, Y. Hu and N. Perrimon, 2018 Pooled genome-wide CRISPR
860 screening for basal and context-specific fitness gene essentiality in Drosophila
861 cells. Elife 7.
862 Yu, Z., M. Ren, Z. Wang, B. Zhang, Y. S. Rong *et al.*, 2013 Highly efficient genome
863 modifications mediated by CRISPR/Cas9 in Drosophila. Genetics 195**:** 289-291.
864

Figure 1

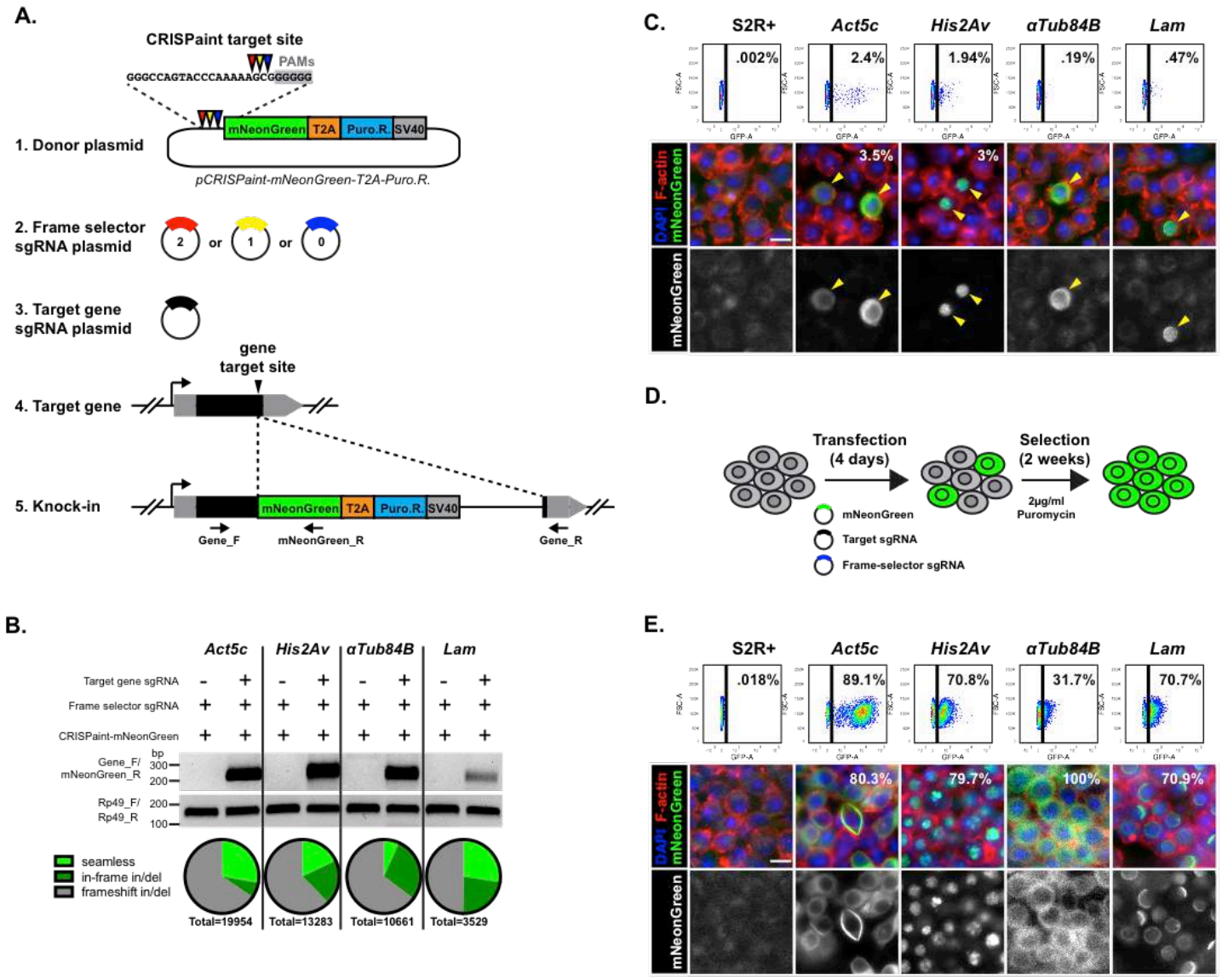

Figure 1 – Knock-in of *mNeonGreen-T2A-PuroR* into Drosophila S2R+ cells using homology-independent insertion. (**A**) Schematic of CRISPaint knock-in approach. *mNeonGreen-T2A-PuroR* is inserted into 3' coding sequence. (**B**) Analysis of knock-in efficiency of transfected cells by diagnostic PCR (DNA gel image) and next-generation sequencing (pie charts). (**C**) Analysis of knock-in efficiency of transfected cells by FACs and confocal microscopy. Numbers indicate percentage of cells with fluorescence. F-actin stained using Phalloidin-TRITC (red), nuclei labeled with DAPI (blue), mNeonGreen signal is in green. Scale bar 10μm. (**D**) Schematic of Puromycin selection of mNeonGreen-expressing cells. (**E**) Analysis of knock-in frequency of puromycin-selected cells using FACs and confocal microscopy. Numbers indicate percentage of cells with green fluorescence. Scale bar 10μm.

Figure 2

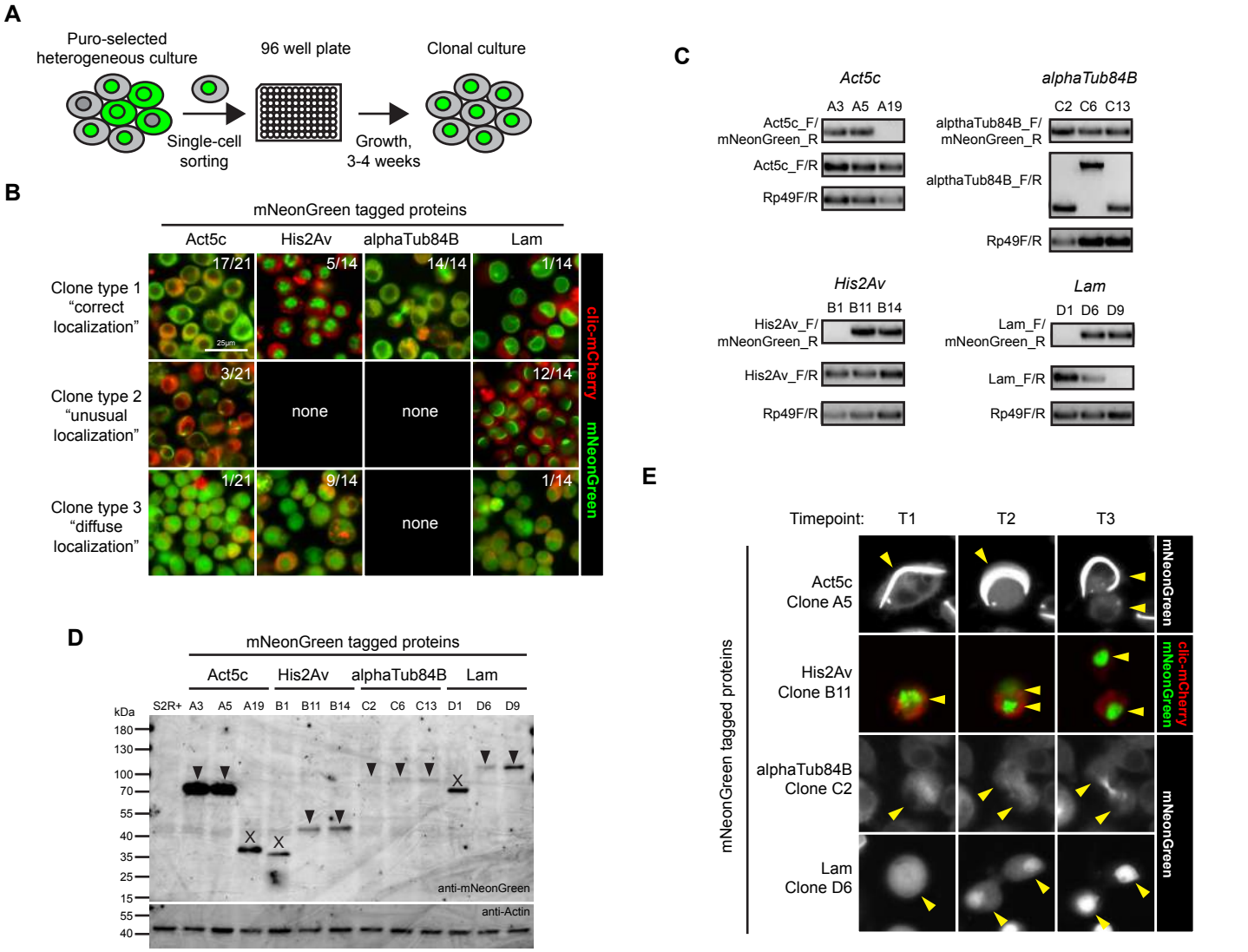

Figure 2. Analysis of S2R+ mNeonGreen-expressing single-cell cloned lines. (**A**) Schematic of FACS isolation of single-cell clones expressing mNeonGreen. (**B**) Confocal images of live mNeonGreen-expressing cell lines, categorized into three clone types. Numbers indicate the frequency of each clone type for each gene targeted. Images show fluorescence from Clic-mCherry (red) and mNeonGreen (green). Scale bar 25µm. (**C**) Agarose gel with PCR fragments amplified from knock-in (Gene_F/mNeonGreen_R) and non-knock-in loci (Gene_F/R). Positive control bands were amplified from *Rp49* genomic sequence. (**D**) Western blot detecting mNeonGreen protein fusions. Arrowheads indicate expected molecular weight. X's indicate incorrect molecular weight. (**E**) Confocal images of live S2R+ cells expressing mNeonGreen protein fusions during cell division at three timepoints. Arrowheads indicate cells before/after cell division.

Figure 3

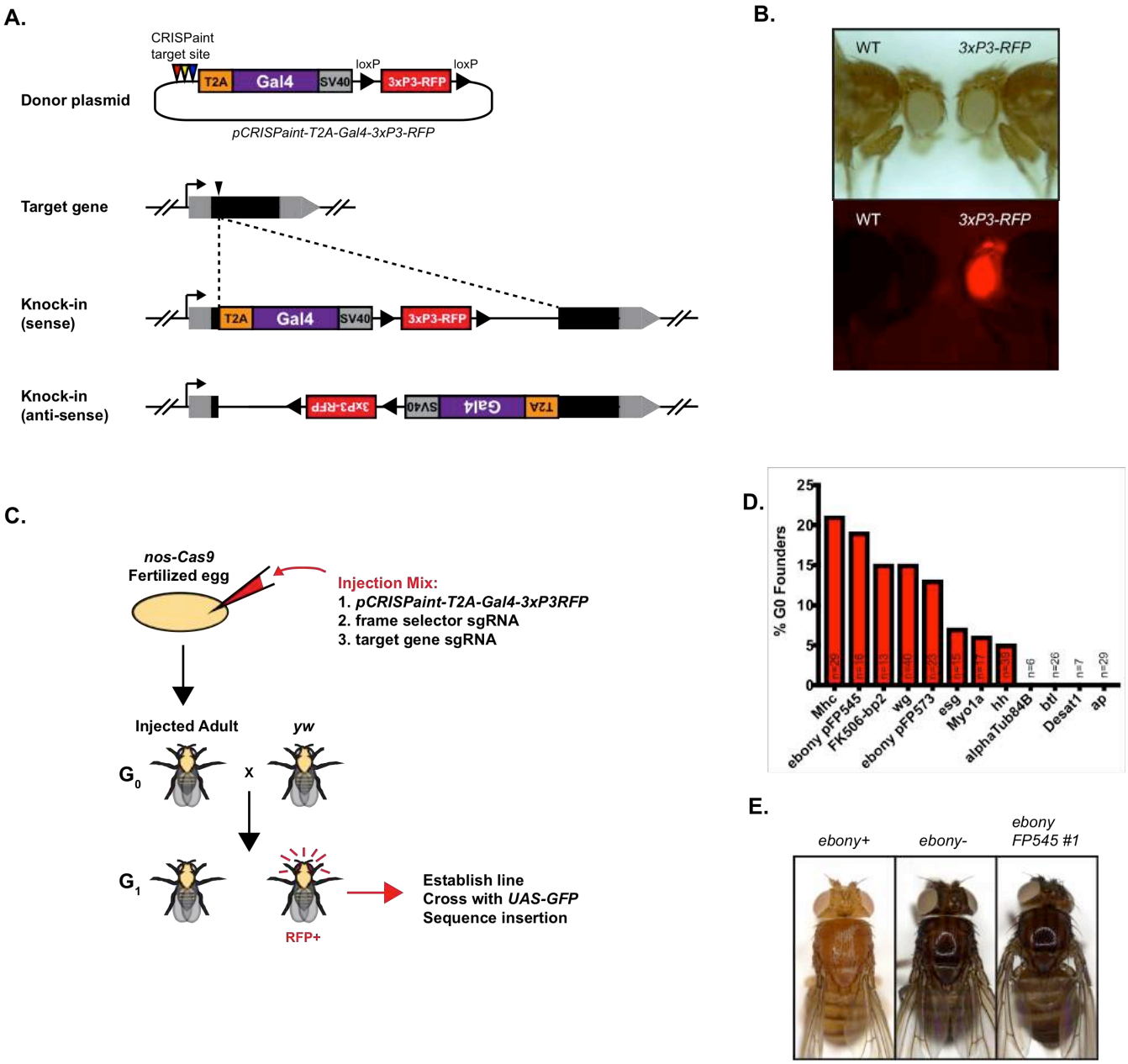

Figure 3 – Knock-in of *T2A-Gal4* into the *Drosophila* germ line using homology-independent insertion. (**A**) Schematic of knock-in approach. *pCRISPaint-T2A-Gal4-3xP3-RFP* is inserted into 5' coding sequence. (**B**) Images of adult flies with 3xP3-RFP fluorescence in the eye. Top panel is brightfield, bottom panel is fluorescence. (**C**) Schematic of plasmid injections, fly crosses, and analysis of insertions. (**D**) Graph with results of knock-in efficiency for 12 sgRNA target sites and 11 genes. (**E**) Image of adult flies. Homozygous *ebony-T2A-Gal4 FP545* #1 flies have dark cuticle pigment.

Figure 4

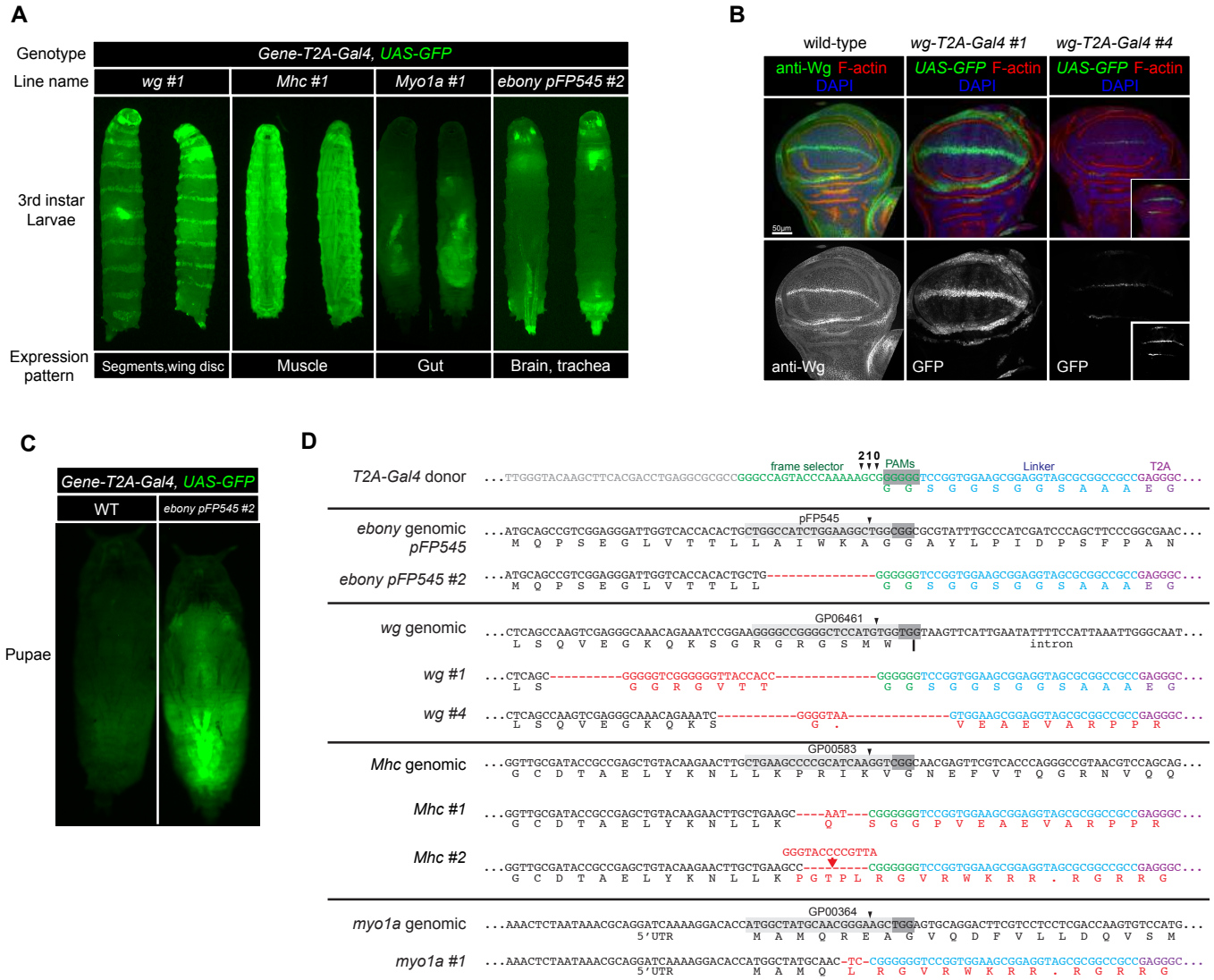

Figure 4 – Germ line insertions that express *T2A-Gal4* under the control of the target gene. (**A**) Fluorescence images of 3rd instar larvae with indicated genotypes. Expression of Gal4 under control of the target gene drives expression of the *UAS-GFP* reporter. (**B**) Confocal images of wing imaginal discs showing protein staining of Wg protein (anti-wg, green) or *UAS-GFP* expression (green). GFP fluorescence was recorded at identical exposure settings for lines *wg-T2A-Gal4* #1 and #4. Inset shows digitally increased GFP signal. Scale bar 50µm. (**C**) Fluorescence image of pupae, *ebony-T2A-Gal4 pFP545* #2 expression is visible throughout the cuticle. (**D**) Sequence structure of *T2A-Gal4* insertions that express Gal4.

Figure 5

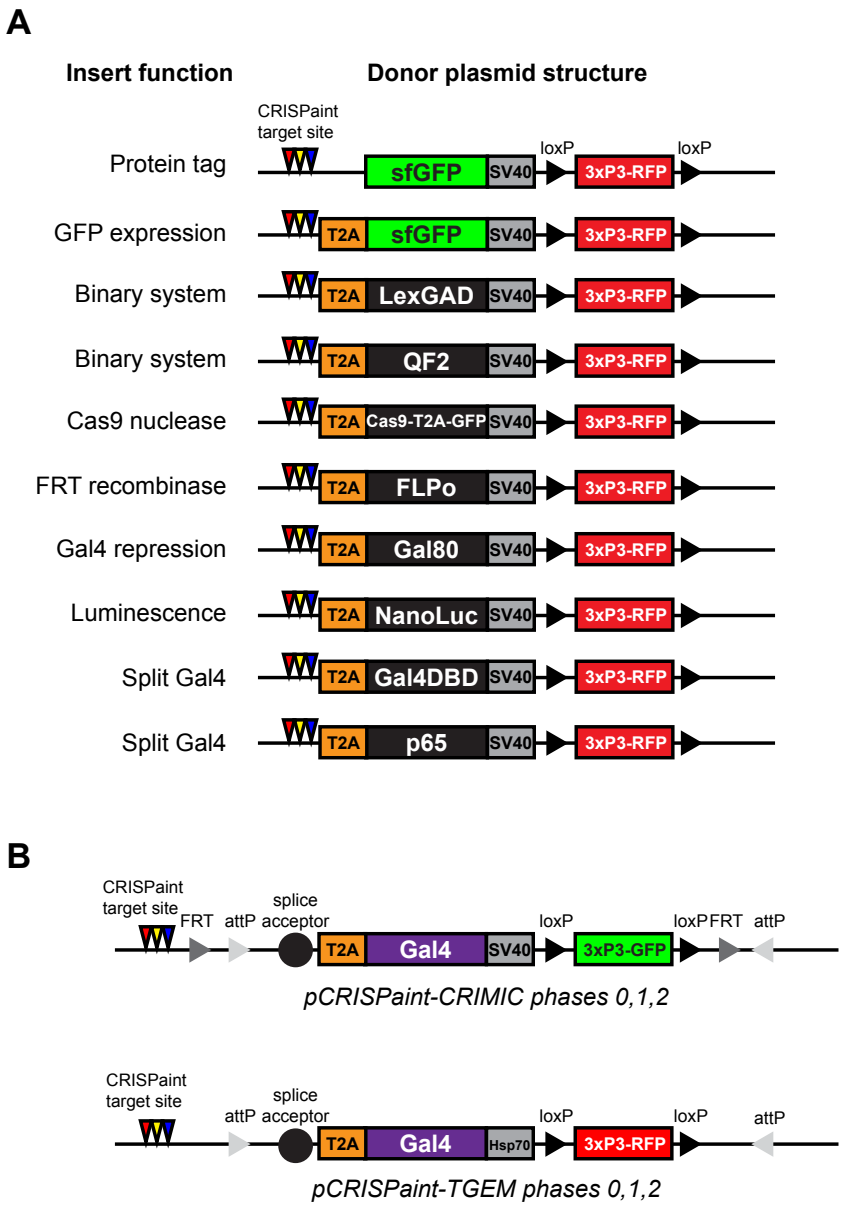

Figure 5 – A collection of CRISPaint-compatible donor plasmids for germ line knock-ins. (**A**) Donor plasmids for insertion into 5' coding sequence. (**B**) Donor plasmids for insertion into intronic sequence, modified from CRIMIC and T-GEM HDR donor plasmids.

Supplemental Figure 1

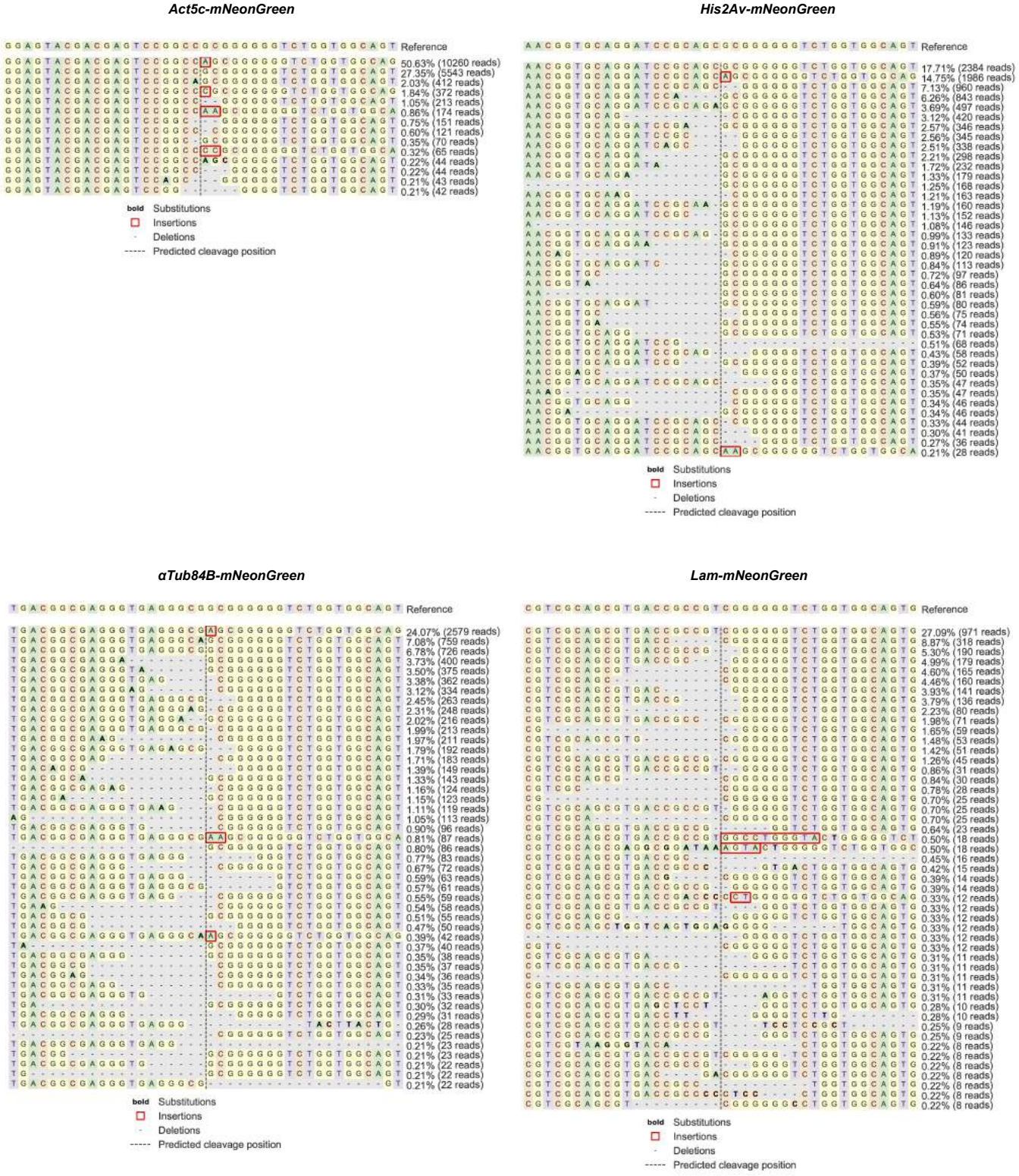

Supplemental Figure 1 – Next-generation sequencing analysis of mNeonGreen insertion sites in transfected S2R+ cells using CRISPresso2

Supplemental Figure 2

Sense insertion

Antisense insertion

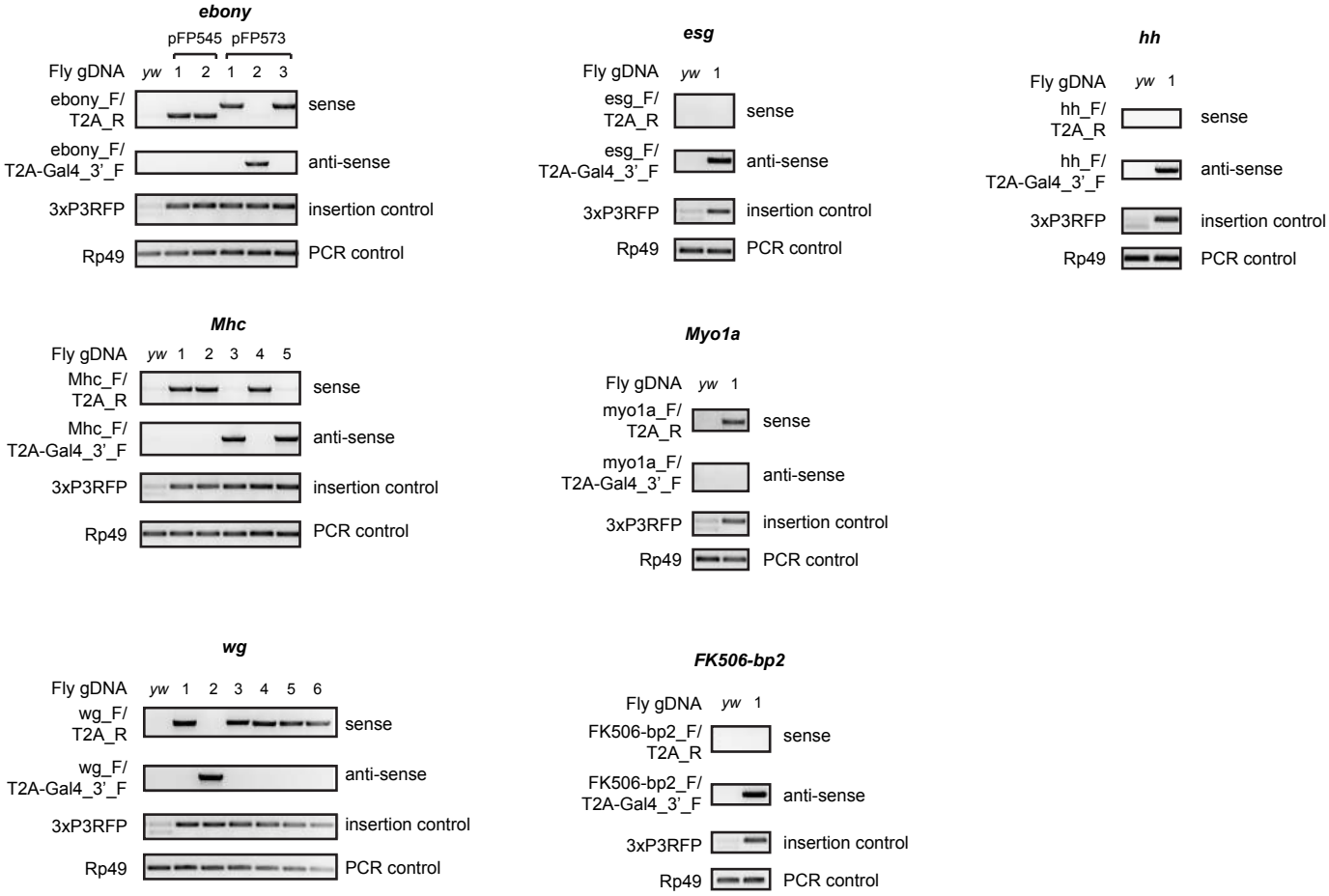

Supplemental Figure 2 – Diagnostic PCR of *CRISPaint-T2A-Gal4* insertions in RFP+ fly lines to confirm their insertion site and orientation.

Supplemental Figure 3

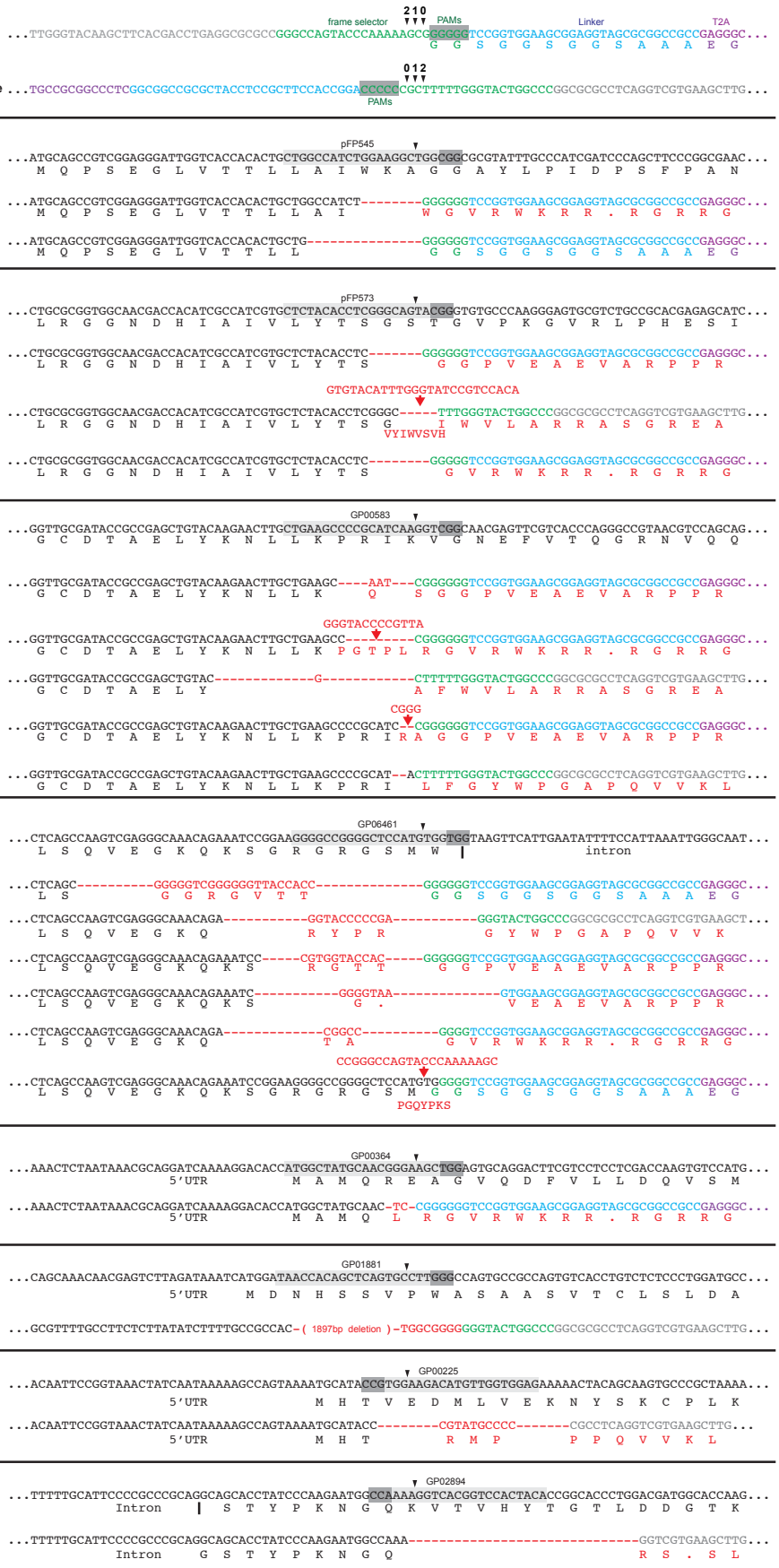

Supplemental Figure 3 – Sequence structure of *CRISPaint-T2A-Gal4* insertions in RFP+ fly lines

Supplemental Figure 4

A

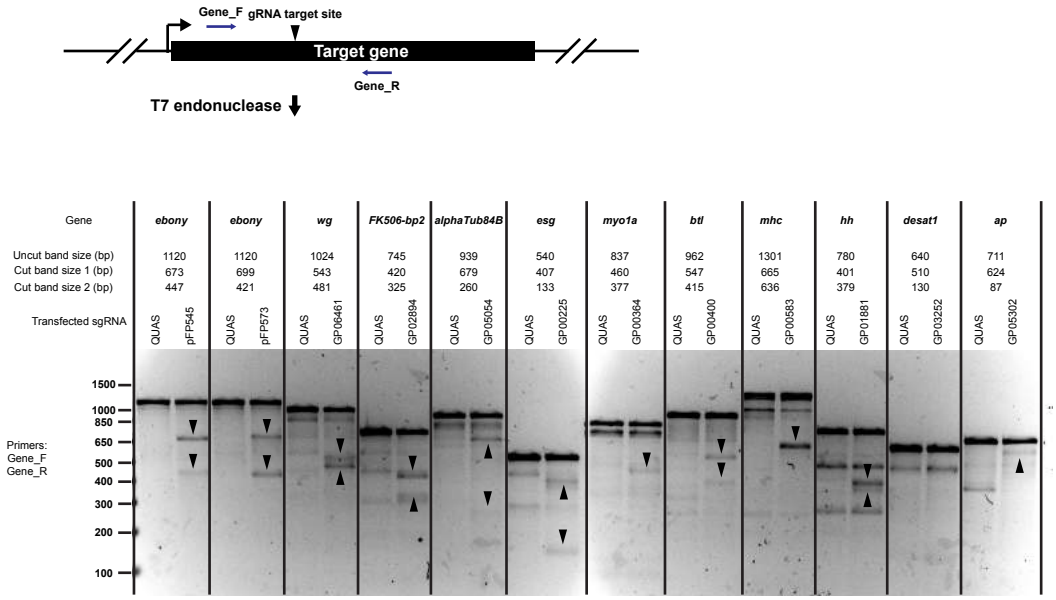

B

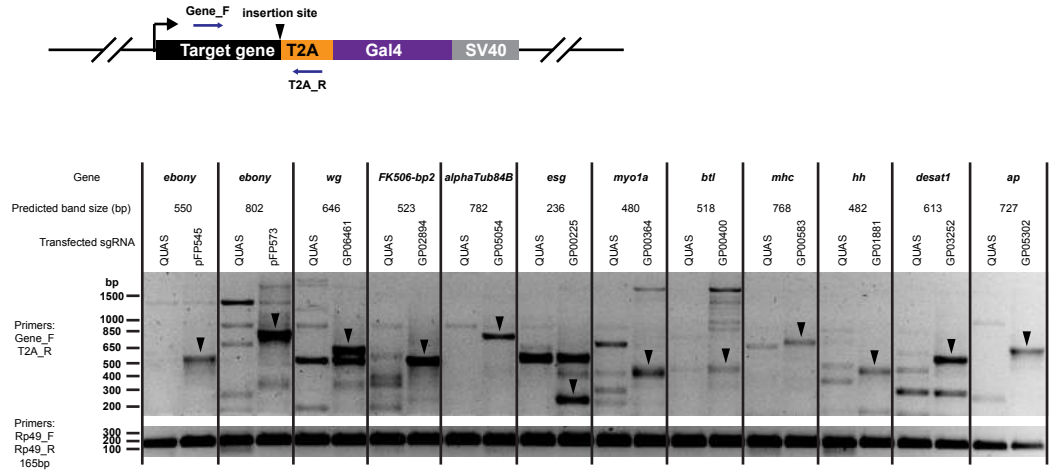

Supplemental Figure 4 – Cutting efficiency of 12 sgRNAs in transfected S2R+ cells. (**A**) T7 endonuclease assay. (**B**) Diagnostic PCR to detect for presence of sense orientation *CRISPaint-T2A-Gal4* insertion events.

	Gene and sgRNA information			
Gene Name	**Protein localization**	**sgRNA plasmid (TRiP)**	**sgRNA target site with PAM**	**frame selector sgRNA**
Act5c	actin	GP07595	GCGGTGCACAATGGAGGGGCCGG	2
His2Av	chromatin	GP07596	GGTGCAGGATCCGCAGCGGAAGG	2
αTub84B	microtubules	GP07609	CGGCGAGGGTGAGGGCGCTGAGG	2
Lamin	nuclear envelope	GP07612	CGCAGCGTGACCGCCGTGGACGG	1
Untransfected				

	CRISPresso2 output			
Gene Name	**seamless**	**in-frame in/del**	**frameshift in/del**	**% in-frame**
Act5c	5543	1343	13068	34.50937155
His2Av	2384	2620	8279	37.6722126
αTub84B	726	3034	6901	35.26873652
Lamin	971	801	1757	50.21252479
Untransfected				

	FACs Transfected			FACs Puro-selected		
Gene Name	**mNeonGreen+**	**Single cells total**	**% mNeonGreen+**	**mNeonGreen+**	**Single cells total**	**% mNeonGreen**
Act5c	1963	80589	2.435816302	45355	50883	89.1358607
His2Av	1554	80291	1.935459765	32780	46298	70.80219448
αTub84B	150	78752	0.190471353	16682	52643	31.6889235
Lamin	385	81688	0.471305455	34826	49234	70.73567047
Untransfected	2	83869	0.002384671	10	55656	0.017967515

	Cell counting transfected (n=6)			Cell counting Puro-selected (n=3)		
Gene Name	**mNeonGreen+**	**Total cells**	**Average % mNeonGreen+**	**mNeonGreen+**	**Total cells**	**Average % mNeonGreen+**
Act5c	17/17/26/18/22/25	571/679/577/599/574/613	3.5	342/280/318	397/398/377	80.3
His2Av	26/21/12/19/13/19	634/634/568/525/669/612	3	314/327/315	397/402/400	79.7
αTub84B				412/400/403	412/400/403	100
Lamin				270/282/259	382/388/374	70.9
Untransfected						

Supplemental Table 1 – Quantification of CRISPaint-mNeonGreen insertion events in transfected and puro-selected S2R+ cells by CRISPresso2, FACs, and cell counting of confocal images.

					endogenous gene			
Clone name	**Gene-mNeonGreen**	**predicted mNeonGreen fusion (kDa)**	**Observed Localization**	**mNeon insertion site**	**allele 1**	**allele 2**	**allele 3**	**allele 4**
A3	Act5c	71.4	very infrequent small rods	seamless	1bp deletion	1bp insertion		
A5	Act5c	71.4	very frequent long rods	seamless	numerous in/dels			
A19	Act5c	71.4	no rods, cyto and nuclear	N/A	numerous in/dels			
B1	His2Av	44.5	cyto and nuclear	N/A	4bp deletion	19bp deletion		
B11	His2Av	44.5	nuclear	seamless	3bp deletion	2bp deletion	1bp deletion	27bp deletion
B14	His2Av	44.5	nuclear	3 bp deletion, 1bp change	19bp deletion	3bp deletion	1bp deletion	
C2	alphatub84B	79.5	mitotic spindles	seamless	wt	6bp deletion	1bp deletion	
C6	alphatub84B	79.5	mitotic spindles	seamless	insertion of 1482bp from alphatub84D			
C13	alphatub84B	79.5	mitotic spindles	3bp deletion	wt	6bp insertion		
D1	Lam	100.9	cytoplasmic, nuclear	N/A	8bp deletion	4bp deletion	3bp insertion	
D6	Lam	100.9	nuclear lamina	seamless	3bp deletion			
D9	Lam	100.9	nuclear lamina, polarized	seamless	N/A			

Supplemental Table 2 – Molecular characterization of single cell cloned mNeonGreen-expressing S2R+ lines.

Gene	Chr.	target gene sgRNA	target site (no PAM)	Frame selector sgRNA	# G0 crosses	# G0 founders	% founders/total	# G1 progeny screened	# G1 RFP+ progeny	% RFP G1/total G1
Mhc	2	GP00583	CTGAAGCCCCGCATCAAGGT	1	29	6	21	2086	21	1.01
ebony	3	pFP545	TGGCCATCTGGAAGGCTGG	1	16	3	19	1298	11	0.85
FK506-bp2	2	GP02894	TGTAGTGGACCGTGACCTTT	1	13	2	15	901	2	0.22
wg	2	GP06461	GGGGCCGGGGCTCCATGTGG	0	40	6	15	4423	26	0.59
ebony	3	pFP573	TCTACACCTCGGGCAGTAC	1	23	3	13	2121	27	1.27
esg	2	GP00225	CTCCACCAACATGTCTTCCA	2	15	1	7	772	1	0.13
Myo1a	2	GP00364	ATGGCTATGCAACGGGAAGC	1	17	1	6	860	1	0.12
hh	3	GP01881	TAACCACAGCTCAGTGCCTT	2	39	2	5	1975	3	0.15
alphaTub84B	3	GP05054	GCTGACGGTAGGTTCCGGTA	1	6	0	0	506	0	0.00
btl	2	GP00400	GGCAAAAGTGCCGATCACGC	2	26	0	0	2085	0	0.00
Desat1	3	GP03252	AAGCTGCAGGAGGACTCCAC	1	7	0	0	386	0	0.00
ap	2	GP05302	CACCACCTGTAGCACATCAA	0	29	0	0	2928	0	0.00

Supplemental Table 3 – Germ line knock-in efficiency of *CRISPaint-T2A-Gal4*

#	Gene targeted	sgRNA	G0 cross #	Insert orientation	Insert frame	Insertion site sequence	Gal4 expression	Homozygous phenotype	Complementation test
1	ebony	pFP545	1	Sense	Out	8bp del	none	dark cuticle pigment	fail to complement e1 on TM3
2	ebony	pFP545	2	Sense	In	15bp del	anterior and posterior trachae in larvae, whole body cuticle in pupae and adult	dark cuticle pigment	fail to complement e1 on TM3
3	ebony	pFP573	1	Sense	Out	7bp del	none	dark cuticle pigment	fail to complement e1 on TM3
4	ebony	pFP573	2	Antisense	N/A	5bp del, 25bp ins	none	dark cuticle pigment	fail to complement e1 on TM3
5	ebony	pFP573	3	Sense	Out	8bp deletion	none	dark cuticle pigment	fail to complement e1 on TM3
6	hh	GP01881	1	Antisense	N/A	1897bp del, 8bp ins	none	lethal	fail to complement hh[AC], Df(3R)ED5296
7	Mhc	GP00583	1	Sense	Out	10bp del, 3bp ins	muscle	lethal	fail to complement P{lacW}Mhck10423, Df(2L)H20
8	Mhc	GP00583	2	Sense	Out	9bp del, 13bp ins	muscle	lethal	fail to complement P{lacW}Mhck10423, Df(2L)H20
9	Mhc	GP00583	3	Antisense	N/A	27bp del, 1bp ins	none	lethal	fail to complement P{lacW}Mhck10423, Df(2L)H20
10	Mhc	GP00583	4	Sense	Out	2bp del, 4bp ins	none	lethal	fail to complement P{lacW}Mhck10423, Df(2L)H20
11	Mhc	GP00583	5	Antisense	N/A	2bp deletion	none	lethal	fail to complement P{lacW}Mhck10423, Df(2L)H20
12	Myo1a	GP00364	1	Sense	Out	4bp del, 2bp ins	gut	viable	complement Df(2L)ED8142
13	esg	GP00225	1	Antisense	N/A	25bp del, 10bp	none	lethal	fail to complement P{enG}esg[G66]
14	FK506-bp2	GP02894	1	Antisense	N/A	30bp del	none	viable	complement Df(2R)Exel6069
15	wg	GP06461	1	Sense	In	45bp del, 21bp ins	wingless, strong expression	lethal	fail to complement wg[I-17], wg[I-8], and Df(2L)BSC291
16	wg	GP06461	2	Antisense	N/A	33bp del, 11bp ins	none	lethal	fail to complement wg[I-17], wg[I-8], and Df(2L)BSC291
17	wg	GP06461	3	Sense	Out	21bp del, 11bp ins	none	lethal	fail to complement wg[I-17], wg[I-8], and Df(2L)BSC291
18	wg	GP06461	4	Sense	Out	32bp del, 7bp ins	wingless, weak expression	lethal	fail to complement wg[I-17], wg[I-8], and Df(2L)BSC291
19	wg	GP06461	5	Sense	Out	28bp del, 5bp ins	none	in progress	fail to complement wg[I-17], wg[I-8], and Df(2L)BSC291
20	wg	GP06461	6	Sense	In	21bp insertion	none	in progress	in progress

Supplemental Table 4 – Molecular and phenotypic characterization of 20 RFP+ fly strains, each carrying a distinct *CRISPaint-T2A-Gal4* insertion.

gene	sgRNA name	sgRNA sequence	DRSC efficiency score
ebony	pFP545	gTGGCCATCTGGAAGGCTGG	5.56968
ebony	pFP573	gTCTACACCTCGGGCAGTAC	5.08877
wg	GP06461	GGGGCCGGGGCTCCATGTGG	5.61857
FK506-bp2	GP02894	TGTAGTGGACCGTGACCTTT	6.5446
alphaTub84B	GP05054	GCTGACGGTAGGTTCCGGTA	6.20359
esg	GP00225	CTCCACCAACATGTCTTCCA	9.35069
Myo1a	GP00364	ATGGCTATGCAACGGGAAGC	7.98579
btl	GP00400	GGCAAAAGTGCCGATCACGC	3.52487
Mhc	GP00583	CTGAAGCCCCGCATCAAGGT	8.00559
hh	GP01881	TAACCACAGCTCAGTGCCTT	6.99912
Desat1	GP03252	AAGCTGCAGGAGGACTCCAC	6.60024
ap	GP05302	CACCACCTGTAGCACATCAA	5.73411

Supplemental Table 5 – Efficiency scores for 12 sgRNAs used in germ line knock-ins

Name	Sequence	How used
JB880_frame+0_gRNA_top	GTCGgccagtacccaaaaagcggg	for cloning pCFD3-CRISPaint_frameselector
JB881_frame+0_gRNA_bot	AAACcccgcttttgggtactggc	for cloning pCFD3-CRISPaint_frameselector
JB882_frame+1_gRNA_top	GTCGggccagtacccaaaaagcgg	for cloning pCFD3-CRISPaint_frameselector
JB883_frame+1_gRNA_bot	AAACccgcttttgggtactggcc	for cloning pCFD3-CRISPaint_frameselector
JB884_frame+2_gRNA_top	GTCGgggccagtacccaaaaagcg	for cloning pCFD3-CRISPaint_frameselector
JB885_frame+2_gRNA_bot	AAACcgctttttgggtactggccc	for cloning pCFD3-CRISPaint_frameselector
JB886_target-T2A-Gal4overlap_gBlock	ttcacgacctgaggcgcgccgggccagtacccaaaaagcgggggggtccggtggaagcggagg tagcgcggccgccgagggccgcggcagcctgctgacctgcggcgatgtggaggagaaccccg ggcccGCTAGCatgaagctactgtcttctatcgaacaagcatgcgatatttgccgacttaaa aagctcaagtgctccaaagaaaaaccgaagtgcgccaagtgtct	gBlock containing CRISPaint site and T2A and overlap sequence
JB877_Gal4_F	atgaagctactgtcttctatcgaaca	to amplify Gal4-3xP3RFP
JB878_target-T2A-Gal4_P3RFP_R	gggaacaaaagctggagctcataacttcgtatagcatacattatacgaagttatCGTATGGG CCTTCGCTGCTTACAG	to amplify Gal4-3xP3RFP
JB915_sfGFP_HIKI_T2A_F	tgtggaggagaaccccgggcccgctagcGTGTCCAAGGGCGAGGAG	for cloning into JAB290 cut with NheI/KpnI
JB916_sfGFP_HIKI_R	caaagatcctctagaggtaccCTACTTGTACAGCTCATCCATGC	for cloning into JAB290 cut with NheI/KpnI
JB1000_LexGAD_HIKI_T2A_F	tgtggaggagaaccccgggcccgctagcATGCCACCCAAGAAGAAGC	for cloning into JAB290 cut with NheI/KpnI
JB1001_LexGAD_HIKI_R	caaagatcctctagaggtaccCTACTCCTTCTTTGGGTTCGG	for cloning into JAB290 cut with NheI/KpnI
JB998_QF2_HIKI_T2A_F	tgtggaggagaaccccgggcccgctagcATGCCACCCAAGCGCAAA	for cloning into JAB290 cut with NheI/KpnI
JB999_QF2_HIKI_R	caaagatcctctagaggtaccTCACTGTTCGTATGTATTAATGTCG	for cloning into JAB290 cut with NheI/KpnI
JB1055_Cas9-T2A-EGFP_HIKI_T2A_F	tgtggaggagaaccccgggcccgctagcATGGATTACAAGGATCACGATG	for cloning into JAB290 cut with NheI/KpnI
JB1056_Cas9-T2A-EGFP_HIKI_R	caaagatcctctagaggtaccTTAGTACAGCTCGTCCATGCC	for cloning into JAB290 cut with NheI/KpnI
JB1002_FLPo_HIKI_T2A_F	tgtggaggagaaccccgggcccgctagcatgagccagttcgacatcct	for cloning into JAB290 cut with NheI/KpnI
JB1003_FLPo_HIKI_R	caaagatcctctagaggtacctcagatccgcctgttgatgtagc	for cloning into JAB290 cut with NheI/KpnI
JB1004_Gal80_HIKI_T2A_F	tgtggaggagaaccccgggcccgctagcATGGACTACAACAAGAGATCTTCG	for cloning into JAB290 cut with NheI/KpnI
JB1005_Gal80_HIKI_R	caaagatcctctagaggtaccTTATAAACTATAATGCGAGATATTGCTAA	for cloning into JAB290 cut with NheI/KpnI
JB1008_Nluc_HIKI_T2A_F	tgtggaggagaaccccgggcccgctagcATGGTCTTCACACTCGAAGATTT	for cloning into JAB290 cut with NheI/KpnI
JB1009_Nluc_HIKI_R	caaagatcctctagaggtaccTTACGCCAGAATGCGTTC	for cloning into JAB290 cut with NheI/KpnI
JB1032_Gal4DBD_HIKI_T2A_F	tgtggaggagaaccccgggcccgctagcATGCTGGAGATCCGCGCC	for cloning into JAB290 cut with NheI/KpnI
JB1033_Gal4DBD_HIKI_R	caaagatcctctagaggtaccTTACGATACCGTCAGTTGCC	for cloning into JAB290 cut with NheI/KpnI
JB1030_p65_HIKI_T2A_F	tgtggaggagaaccccgggcccgctagcATGGATAAAGCGGAATTAATTCC	for cloning into JAB290 cut with NheI/KpnI
JB1031_p65_HIKI_R	caaagatcctctagaggtaccTTACTTGCCGCCGCCCAG	for cloning into JAB290 cut with NheI/KpnI
JB917_sfGFP_HIKI_F	ggtggaagcggaggtagcgcggccgccGTGTCCAAGGGCGAGGAG	for cloning into JAB290 cut with NotI/KpnI
JB916_sfGFP_HIKI_R	caaagatcctctagaggtaccCTACTTGTACAGCTCATCCATGC	for cloning into JAB290 cut with NotI/KpnI
JB969_crispaintsite_NsiI_top	agggccagtacccaaaaagcgggggggtTGCA	for cloning into CRIMIC pM37
JB970_crispaintsite_NsiI_bottom	acccccccgcttttgggtactggccctTGCA	for cloning into CRIMIC pM37
JB971_crispaintsite_AgeI-NotI_top	ccggtgggccagtacccaaaaagcgggggggc	for cloning into T-GEM
JB972_crispaintsite_AgeI-NotI_bottom	ggccgccccccgcttttgggtactggccca	for cloning into T-GEM
JB1355_FK506-bp2_geno_1F	acgcgccaaaatacaaaaac	amplification of endogenous target gene and knock-in
JB1356_FK506-bp2_geno_1R	GCCTATTCGACCTTGAGCAG	amplification of endogenous target gene
JB1357_alphaTub84B_geno_1F	tttgtgtgggcaaaattcaa	amplification of endogenous target gene and knock-in
JB1358_alphaTub84B_geno_1R	GCTTGGACTTCTTGCCGTAG	amplification of endogenous target gene
JB1359_esg_geno_1F	CGTTTGGTATTTGTGCATCG	amplification of endogenous target gene and knock-in
JB1360_esg_geno_1R	GTAGGGCGACATGTGGAAGT	amplification of endogenous target gene
JB1361_btl_geno_1F	aactaagggaggggcaaaaa	amplification of endogenous target gene and knock-in
JB1362_btl_geno_1R	CGTCCACCAAGGATTTGAGT	amplification of endogenous target gene
JB1363_Desat1_geno_1F	aatccacctggtgcttgttc	amplification of endogenous target gene and knock-in
JB1364_Desat1_geno_1R	GTAACCGAAGGCGATGATGT	amplification of endogenous target gene
JB1365_ap_geno_1F	ttgcaaatctgtcaggaacg	amplification of endogenous target gene and knock-in
JB1366_ap_geno_1R	ATCTGGACACGAGGATGAGG	amplification of endogenous target gene
JB959_ebony_geno_F	gcattagcctgcattgcata	amplification of endogenous target gene and knock-in
JB960_ebony_geno_R	CACGCCCTCATCGAAATAGT	amplification of endogenous target gene
JB961_wg_geno_F	CAGTTAAGCGTTGGCACTGA	amplification of endogenous target gene and knock-in
JB962_wg_geno_R	ttgttgcatctctgcggtag	amplification of endogenous target gene
JB963_Myo1a_geno_F	TCGTCGTCATCAACAGAAGC	amplification of endogenous target gene and knock-in
JB964_Myo1a_geno_R	tctggagtggaaccgaaaac	amplification of endogenous target gene
JB965_Mhc_geno_F	cggctaaagactgacccaaa	amplification of endogenous target gene and knock-in
JB966_Mhc_geno_R	CTCTTGCTCCATGACGAACA	amplification of endogenous target gene
JB967_hh_geno_F	TCGTACTCGCACTCGAACAC	amplification of endogenous target gene and knock-in
JB1388_hh_geno_6F	aaatcaaagctggaccaaatc	amplification of endogenous target gene and knock-in, used with hh #1 insertion
JB968_hh_geno_R	GTTGTAGTTGGGCACGAGGT	amplification of endogenous target gene
JB900_T2A_R	cggggttctcctccacat	reverse primer for amplifying T2A-Gal4 insert in sense orientation
JB958_T2A-Gal4_3'_F	gttttcccagtcacgacgtt	reverse primer for amplifying T2A-Gal4 insert in antisense orientation
JB659_3P3dsred_seq1F	ACTCCAAGCTGGACATCACC	to amplify 3xP3-dsred as a control
JB660_3P3dsred_seq1R	CGAGGGTTCGAAATCGATAA	to amplify 3xP3-dsred as a control
JB713_Rp49_F	ATCGGTTACGGATCGAACAA	to amplify endogenous Rp49 gene as a control
JB714_Rp49_R	GACAATCTCCTTGCGCTTCT	to amplify endogenous Rp49 gene as a control
JB1051_alphaTub84B_C-term_F	CCTTCGTCCACTGGTACGTT	amplification of endogenous target gene and knock-in
JB1052_Act5c_C-term_F	CGTCGACCATGAAGATCAAG	amplification of endogenous target gene and knock-in
JB1053_His2Av_C-term_F	CTCCTCGCCACTTACAGCTC	amplification of endogenous target gene and knock-in
JB1054_Lam_C-term_F	GCCGACAACACTAGGACGAT	amplification of endogenous target gene and knock-in
JB1050_mNeonGreen_R	GGGAGAGAGGCGTTATCCTC	reverse primer for amplifying gene-mNeonGreen insert
JB1120_act5c_seqnextgenR	CGACTTCTCCTCCTCCTCCT	amplification of endogenous target gene
JB1121_His2av_seqnextgenR	TCGTCGGTGTTTTAGCTTGTC	amplification of endogenous target gene
JB1122_alphatub_seqnexgenR	GCGATTGGAAGCGTAAACAC	amplification of endogenous target gene
JB1123_Lam_seqnextgenR	GTGTTGTGCTGCGTTTGATT	amplification of endogenous target gene
JB1192_Lam_2F	GCGGCTAATCAACGAGAAAG	amplification of non-knock-in Lamin gene
JB1193_Lam_2R	TCTGTTGTCAGGAGCGTTTG	amplification of non-knock-in Lamin gene
JB1194_Lam_3F	ACGAGGAGCAGATGCAGATT	amplification of non-knock-in Lamin gene
JB1195_Lam_3R	GGTCTAAACCGGGAGAAAGC	amplification of non-knock-in Lamin gene
JB1196_Lam_4F	AGCTGCAGAACCTGAACGAT	amplification of non-knock-in Lamin gene
JB1197_Lam_4R	ACTAGCCGAACCCAGGATTT	amplification of non-knock-in Lamin gene
JB1198_Lam_5F	cccattacaagcgacgattt	amplification of non-knock-in Lamin gene
JB1199_Lam_5R	GAACAGCTCCACTCCTCCAG	amplification of non-knock-in Lamin gene
JB1200_Lam_6F	GTCTCGGTCTGCTCCTCATC	amplification of non-knock-in Lamin gene
JB1201_Lam_6R	GAATGGCATAGCCACCACTT	amplification of non-knock-in Lamin gene
JB1202_Lam_7F	CATTTGCAAGATGGTGGTTG	amplification of non-knock-in Lamin gene
JB1203_Lam_7R	ccaattaggccaacactgct	amplification of non-knock-in Lamin gene
JB1050_mNeonGreen_R	GGGAGAGAGGCGTTATCCTC	amplification and sequencing primer, 5' end of mNeonGreen

Supplemental Table 6 – Oligo and dsDNA sequences